scientific reports



OPEN

Investigation of flexural mechanical and creep properties of sleeve reinforced pultruded glass fibre reinforced polymer composite for crossarm application

Vijayvignesh Namasivayam Sukumaar^{1⊠}, Mohamad Ridzwan Ishak^{1,2,3™}, Mohd Na'Im Abdullah¹, Mohamed Yusoff Mohd Zuhri^{3,4} & Muhammad Asyraf Muhammad Rizal^{5,6}

Pultruded glass fiber-reinforced polymer (PGFRP) composites are innovative materials used in high-rise transmission towers that undergo failure due to long-term static loading phenomenon. This research focuses on retrofitting PGFRP composite cross-arms with plug-in type sleeve reinforcements by employing a three-point bending (3 PB) test to analyze the cross-arm's elastic properties, flexural creep response, and deflection behaviour. The addition of the sleeve retrofit significantly improved the load-deflection behaviour and long-term creep resistance, by 45.30% and 47.10%, respectively. Findley's power law model was used to accurately predict the viscoelastic response of the structure, revealing that the virgin cross-arm experienced a 75% drop in elastic modulus, while the sleeve-reinforced cross-arm saw only a 34% decrease indicating over 40% improvement in the cross-arm's ability to resist deformation over extended periods. Additionally, the overall reduction factor improved by 0.51 in contrast to virgin cross-arm. The sleeve-reinforced cross-arm showed reduced deflection, better creep resistance, increased bending strength, and a longer theoretical lifespan. Predictions indicate that the improved cross-arm surpasses the current one in long-term mechanical performance.

Keywords Cross-arm, Sleeve, Flexural properties, PGFRP composite, Elastic moduli

The transmission towers in Malaysia employed wooden cross-arms during the initial establishment of power lines¹. Figure 1 illustrates the various parts of the transmission tower. One of the key component of the transmission tower that suspends the utility wires and insulators are known as cross-arms, ensuring that the wires are kept safely above the ground. These cross-arms were first employed in 1929 upon 66 kV towers made of *Neobalanocarpus*, commonly referred to as Chengal wood. In 1963, their use was expanded to 132 kV suspension towers. By the late 1990s, it was hard to acquire wood that could be utilized to create cross-arms of high quality since cross-arms made of wood succumbed to weathering due to ageing. Furthermore, these cross-arms started to disintegrate just after 14 years of use due to natural wood flaws, which was shorter than the expected service life²-⁴. Pultruded glass fiber-reinforced polymer (PGFRP) composite, a lightweight and highly durable alternative to wood, was used to preserve the sustainability of non-conductive cross-arms⁵⁻⁸.

The pultrusion manufacturing technology was chosen for these composite structures because its capability for large scale production and provision of better mechanical qualities than wood^{9–11}. The E-glass fibres wetted with

¹Department of Aerospace Engineering, Universiti Putra Malaysia (UPM), 43400 Serdang, Selangor, Malaysia. ²Aerospace Malaysia Research Centre (AMRC), Universiti Putra Malaysia (UPM), 43400 Serdang, Selangor, Malaysia. ³Laboratory of Biocomposite Technology, Institute of Tropical Forestry and Forest Products (INTROP), Universiti Putra Malaysia (UPM), 43400 Serdang, Selangor, Malaysia. ⁴Advanced Engineering Materials and Composites Research Centre (AEMC), Department of Mechanical and Manufacturing Engineering, Universiti Putra Malaysia (UPM), 43400 Serdang, Selangor, Malaysia. ⁵Engineering Design Research Group, Faculty of Mechanical Engineeting, Universiti Teknologi Malaysia, 81310 Johor Bahru, Johor, Malaysia. ⁶Centre for Advanced Composite Materials (CACM), Universiti Teknologi Malaysia, 81310 Johor Bahru, Johor, Malaysia. [∞]email: n.s.vijayvignesh@qmail.com; mohdridzwan@upm.edu.my

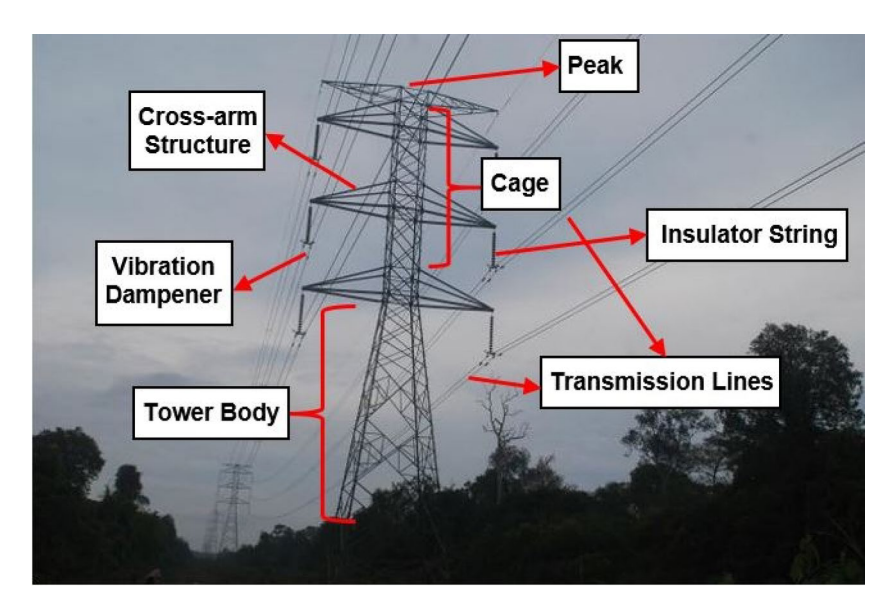


Fig. 1. Various parts of a transmission tower⁴.

Cross-arm problems	Proposed solutions	Ref.
Corrosion and ageing of steel & wooden cross-arms subjected to environment	Adoption of glass fibre reinforced polymer composite material	25,26
Higher self-weight of cross-arms	Introducing variations in fibre laminate stacking and raster angles	11,27
Reduced durability of cross-arm over longer time period	Incorporation of bracing fixtures encompassing tie and main members	28,29
Redundancy in structural reinforcement and higher slip potential	Install honeycomb structure and filament winding at critical point	30-35
Increased slackness of electrical lines due to higher offset of cross-arms	Fasten the cross-arms to body of the tower	36
Practical loads and varying environmental conditions deflate the mechanical properties	Utilize hybrid natural fibre or filled-honeycomb sandwich structure reinforced polymer composite	37

Table 1. Overview of past research related to cross-arms.

unsaturated polyester resins were pultruded to create the cross-arm components on account of their desirable qualities such as being affordable, robust, lightweight and corrosion resistant¹². Due to its symmetrical square tube design, they possess excellent static loading properties and is anisotropic. When compared to alternative fibre orientations, the longitudinal direction of the PGFRP composite cross-arm design exhibits a noticeably stronger mechanical performance.

The primary issue that researchers noticed after some time of operation was the high-rise transmission tower's PGFRP composite cross-arm's sudden breakdown^{11,13}. Common mechanical problems include cable breakage, creep, large temperature and humidity fluctuations, vibration, and dynamic loads like wind^{14–16}. This rapid deterioration can disrupt the electrical transmission and increase the electrical provider's maintenance costs¹⁷. The electrical conductor lines will be drawn closer to the ground by the broken cross-arm, and this exposure can lead to fatality to by-walkers and other infrastructure^{10,18,19}. Low fibre bonding and stacking sequence^{20,21}, compression and tension failure²², and low material creep^{23,24} are some of the factors that have been linked to the cause of an abrupt failure. Table 1 lists a number of compilations of cross-arm problems that have been recognized along with suggested fixes that have been thoroughly examined by multiple research.

Creep behaviour refers to the time-dependent deformation of a material when subjected to a constant load or stress over an extended period. Unlike instantaneous elastic deformation, creep occurs gradually and can lead to significant dimensional changes or mechanical degradation under sustained service conditions. This phenomenon becomes particularly critical in polymer-based materials and their composites, such as GFRP, due to the viscoelastic nature of the polymer matrix²³. In the context of GFRP composites used for structural applications, such as bridge decks, beams, marine structures, and reinforcing bars, the assessment of creep behaviour is of great importance. These materials are often exposed to prolonged loading conditions in real-world scenarios, including static mechanical loads, environmental conditions such as temperature and humidity, and cyclic/dynamic operational loads²⁴. If the time-dependent deformation is not adequately accounted for, it can compromise the dimensional stability, load-bearing capacity, and long-term safety of the structure. Furthermore, the anisotropic and heterogeneous nature of GFRP composites means that creep behaviour does not occur uniformly across different loading directions or environmental conditions. Studying this behaviour enables engineers and material scientists to predict the service life more accurately, develop reliable design models, and implement appropriate safety factors in structural applications. By investigating creep mechanisms in GFRP, including matrix flow, fibre-matrix debonding, and microstructural damage accumulation, researchers

can enhance the material formulation and optimize composite architecture for better performance and durability¹⁴. Thus, understanding creep behaviour is not only fundamental for structural reliability but also essential for advancing sustainable and cost-effective composite design in civil infrastructure.

The failure of cross-arm structures is a significant issue, yet effective solutions remain elusive. At present, the primary approach to addressing the sustainability challenges of PGFRP composite cross-arms involves temporary strengthening with additional structural components. To prolong their service life, one such strategy is the installation of bracing fixtures^{28,29}. However, these bracing systems present difficulties in terms of installation, repair, and maintenance. Additionally, they can lead to slippage due to the immense load they place on the beams, and their design redundancy could result in catastrophic failure. Furthermore, these systems often incorporate wooden components, which deteriorate more rapidly than the composite material, rendering them unsuitable for prolonged use. Another technique employed involves bonding honeycomb sandwich structures to the outer surfaces of PGFRP composite cross-arms^{30,31}. These honeycomb reinforcements are attached using polyester resin, but factors like heat, moisture, and ultraviolet (UV) light can degrade the resin, weakening its mechanical properties and adhesive strength, ultimately increasing the risk of failure of the reinforcement^{38–40}.

Metamaterials with negative Poisson's ratio offer a way to build even-numbered modules into polygons with pivots³⁹. This contribution to the latest material design advancements expands design possibilities for various applications by strategically eliminating hinges to create fully deployable structures. Their parametric study explores how different variables influence mechanical properties and fatigue lifespan⁴⁰. In the meantime, another study uses techniques like group theory and the bar-hinge model to investigate the multi-stability of a hexagonal origami hyperar, which identifies stable configurations and parameters that influence the transitions between these states⁴¹. Researchers concentrate on the creep response of GFRP pultruded flexural components to understand their long-term behaviour. This study focused on analyzing GFRP deck panels over a 5-month period. By simulating creep behaviour, it led to identification of inconsistencies in design standards⁴². Numerous studies have also proposed modifications to the design in order to prevent or lessen such deteriorations^{43,44}. There is currently a dearth of basic research on proposing a unique design for desired use in such members.

The literature shows that although PGFRP composite cross-arms outperform wooden beams, they still face sustainability issues. These cross-arms lose mechanical integrity over time due to environmental exposure, with stress from transmission lines and weather elements contributing to failures. Current solutions, such as temporary bracing or honeycomb panels, are short-term fixes. These methods are costly, require skilled labour, and do not address the buckling failure, which arises due to the slenderness of the cross-arm member. In addition, the fact that the failure of the cross-arm is a point phenomenon, as described by the previous research works, is void as such long structures subjected to dynamic loads for longer duration causes uneven stresses along the critical region rather than at a critical point. Structural strengthening needs to be suitably adopted so as to counter all of these mentioned drawbacks along with the feasibility of incorporation.

Thus, this study will look into the possibility of employing plug-in type sleeve reinforcements. The structural sleeve reinforcement aims not only to offer a practical solution by enhancing structural strength but also to form a unified component that limits cross-arm deflections along both vertical and horizontal axes, ultimately increasing its operational lifespan. In order to improve the cross-arms by installing sleeves, the numerical deformation behaviour was examined²⁸ and other similar mechanical experimental research works upon polymer composite beams to understand the failure modes^{45,46}.

Another objective of this project is the creation of novel plug-in type sleeve reinforced composite cross-arm structures, with an emphasis on the load-bearing capacities and durability of high-rise transmission towers. The construction industry frequently uses sleeve installations because of their effectiveness in reinforcing and connecting essential portions between beams, columns, and other structurally different connections with a loading pattern akin to that of the cross-arms^{47,48}. As a result, the sleeves may provide the required load-sustaining capacity in long-term applications while avoiding yielding that could result in rupture.

The flexural behaviour of sleeve constructions has been thoroughly studied by researchers, who have looked at a number of variables, including material stiffness and bending resistance. Research has evaluated the flexural characteristics of sleeve reinforced polymer composite beams^{49–51}. Flexural behaviour information is necessary for characterization procedures to evaluate a material's appropriateness for practical uses. Three-point bending tests have been utilized in studies to validate the mechanical behaviour of various composite sleeved beams, to understand the impact of physical dimensions in adjusting flexural properties, and explore novel designs for enhanced performance^{52–54}.

In order to increase load-carrying capacities, recent research has focused on optimizing sleeve constructions through creative designs, material selection, and parameter optimization^{55–57}. The importance of taking local denting effects into account in theoretical assessments is highlighted by the inherent consistency⁵⁸. Furthermore, studies on sleeve constructions have shown that they are more capable of absorbing energy and supporting loads than their virgin counterpart. Research also looks at creep behaviour to understand material reactions and mechanisms under constant static loads^{59–61}. Recent creep analysis studies evaluate creep performance in tropical regions using both applied and theoretical methods^{62–64}.

The response of sleeve-reinforced PGFRP composite cross-arms in 132 kV transmission towers to flexural load-deflection and flexural creep remains unexplored. Moreover, no research specifically examines the flexural behavior of cross-arms strengthened with sleeves. The characteristics of full-scale PGFRP composite cross-arms are not fully covered in the majority of the literature and are found to be limited at the coupon size level. In order to provide an empirical model and experimental data of a full-scale sleeved PGFRP composite cross-arm, this study presents analysis of sleeve retrofitted cross-arm structures that offers insights upon their development. By employing such techniques, this study aims to shed more light on the importance of the sleeved structure in structural applications.

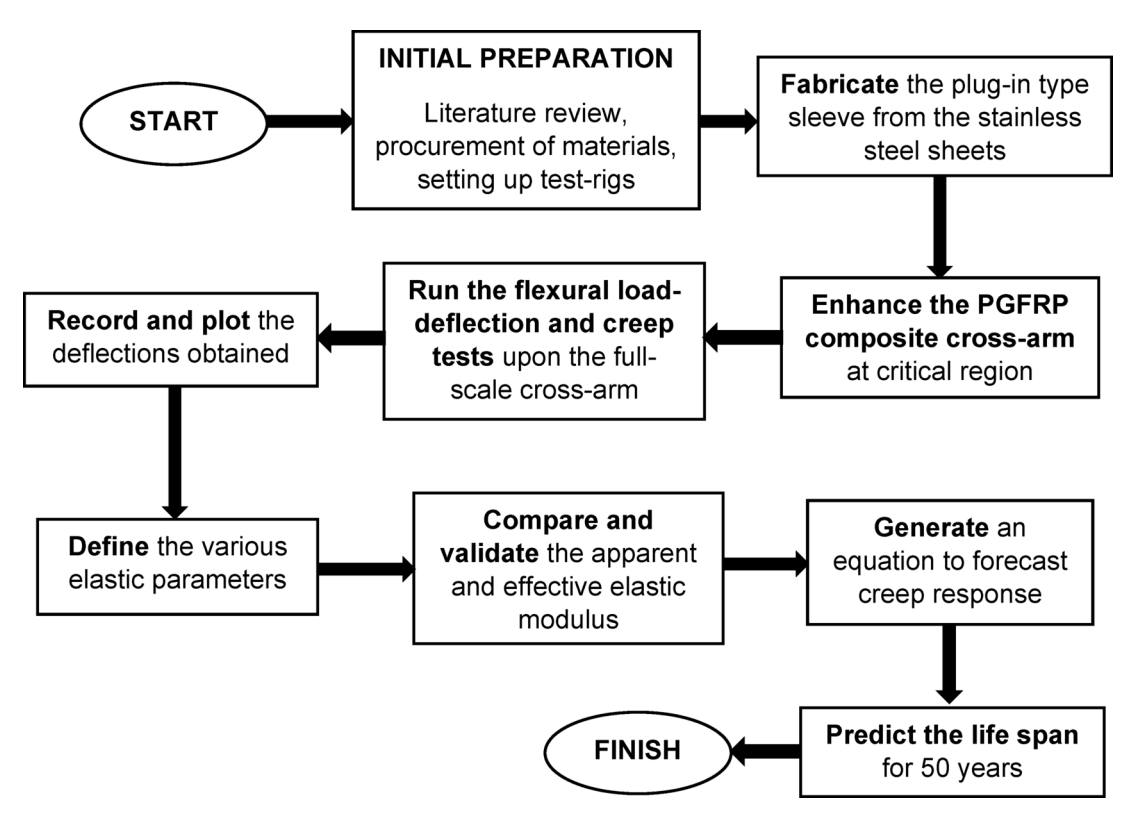


Fig. 2. Flowchart of research activities.

Property	PGFRP composite
Density	2580 kg/m³—E-glass 1350 kg/m³—Unsaturated polyester
Texture	Fine, homogenously and unidirectional fibre along the matrix
Shrinkage	Low
Natural Durability	Low
Modulus of Elasticity	29.8 GPa
Modulus of Rupture	858.0 MPa

Table 2. Properties of PGFRP composite^{65,66}.

Methodology

The research methodology used in this study can be essentially categorized into two groups: numerical analysis and experimental works. The detailed investigations of this study are discussed in the sections that follow. Figure 2 displays the flowchart for the integrated methodology.

Materials

Initially, the plug-in type sleeve is fabricated and then integrated onto the PGFRP composite cross-arm member manufactured by Electrius Sendirian Berhad, Malaysia. The cross-arm's $102 \times 102 \text{ mm}^2$ square cross-section and 7.8 mm wall thickness with a total length of 3651 mm meets the specifications set forth by the multinational electricity company Tenaga Nasional Berhad (TNB), Malaysia. Its unidirectional, miniscule fibre texture is consistent with polymer matrix composites 5,14 . Table 2 and Table 3 respectively displays the full-scale cross-arm main member specifications and the standard-compliant attributes of the utilized PGFRP composite.

The adoption of particular configuration of composites is due to the many positive implications at each laminate level. Varying the fibre orientations could help enhance the flexural strength and damage resistance. These orientations are frequently used in real-world applications where composites experience multi-directional loading⁶⁹. The layer thicknesses variations have direct influence on the composite's stiffness and load transfer capabilities. Thicker layers are anticipated to improve load-bearing capacity, while thinner layers may enhance flexibility and damage resistance. By alternating different thicknesses, the overall mechanical performance could be improved⁷⁰. The configurations were chosen to reflect a range of practical design scenarios, where varying stacking sequences and layer thicknesses are used based on specific load conditions and performance needs. These

Material	Resin	Fibre
Composition		
PGFRP Composite	Unsaturated polyester (UPE) (63 vol. %)	E-glass fiber (37 vol. %)
Composite layer	Orientation (°)	Thickness (mm)
Parameters		
First (outer)	45	0.5
Second	-45	0.5
Third	90	0.7
Fourth	0	3.6
Fifth (Inner)	45	0.7

Table 3. Parameters of PGFRP composite^{67,68}.

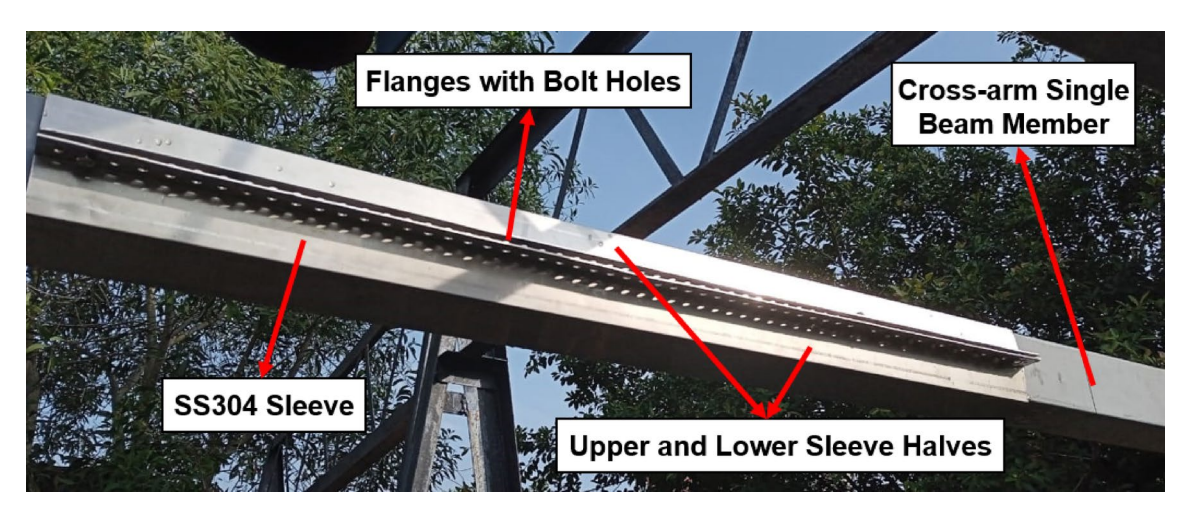


Fig. 3. Sleeve mounted with a transition fit before fastening.

configurations help identify the optimal combinations of stacking sequence and layer thickness for particular applications. By testing various configurations, the aim to simulate real-world composite structures and gain a deeper understanding of how these parameters interact to affect performance under load were materialized.

The structural grade stainless steel SS304-2B sheets were purchased from Tan Central Metal Sendirian Berhad, Malaysia, in order to fabricate the sleeve reinforcement. The length of the sleeve reinforcement was kept constant throughout the study at 1200 mm, or roughly one-third of the cross-arm's total length⁶³. The sleeves were made as two symmetrical halves that encompass all the faces of the PGFRP composite cross-arm with flanges. This plug-in type reinforcement integrates directly into existing cross-arm members without requiring disassembly of the structure. Although the electrical conductivities of the materials employed are not the focus of the study, stainless steel was chosen since it is significantly less conductive than the mild steel and aluminium that were previously utilized as reinforcement^{28–31}. Furthermore, the 1.5 mm thick silicone rubber sheets were used to insulate the interface between the PGFRP composite cross-arm and sleeve. These sheets also serve as a water-proof medium and lessen the possibility of slippage.

The sleeve is fastened to the cross-arm main parts. The silicone rubber was added to create a cushioning effect^{71,72}. Since the mid-point of the cross-arm is the critical area of failure, the two sleeve halves are positioned symmetrically to provide a transition fit^{29,31}. The bolting of the sleeves were done wherein the spring washers absorb shock by providing an axial load that counteracts vibrations, whereas flat washers evenly disperse the fastener's load^{73,74}. The fine threaded bolt guarantees a higher strength of reinforcement in both shear and tension because of its broad contact area⁷⁵. Figure 3 shows the transition fit sleeve mounted PGFRP composite cross-arm.

Experimental setup

Three-point bending (3 PB) loading condition, as per ASTM D790 and ASTM D2990 standards, were employed along the longitudinal direction to analyze the elastic bending properties of a single cross-arm main member under instantaneous and creep loads respectively 76,77. The induced load on the cross-arm member was measured using a 3-ton crane scale. To record the generated deflection, an analogue dial gauge (Mitutoyo 2050A, Japan) was placed at the centre of the loading hook on the cross-arm member, as shown in Fig. 4. The creep tests were conducted in outdoor environment to mimic the actual operational conditions.

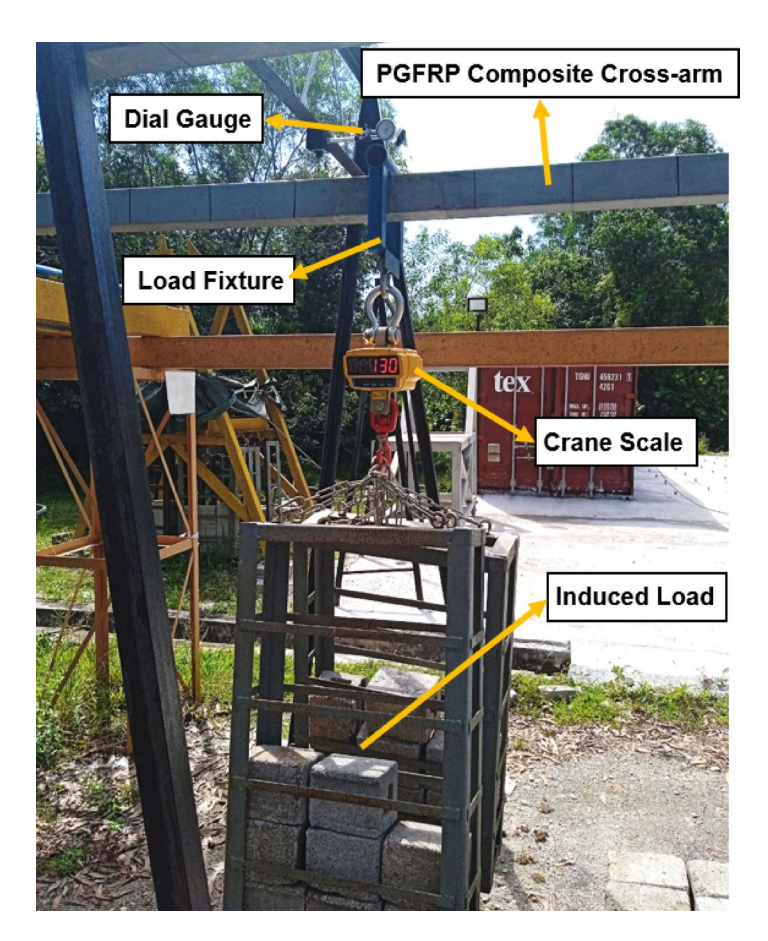


Fig. 4. Single beam PGFRP composite cross-arm under three-point bending condition.

Flexural load-deflection experiment

The PGFRP composite was considered as an anisotropic material. Thus, in this investigation, the equation of beam deflection that takes into consideration the impact of shear deformation, for pultruded fiber-reinforced members, was applied⁷⁸. The cross-arm members were loaded over five distinct span lengths, namely, 1000 mm, 1500 mm, 2500 mm, and 3000 mm. This condition was applied to both the virgin and sleeve reinforced PGFRP composite cross-arm member to observe a comparative analysis by applying the methodology from the previous research³¹. Equation (1) provides the relation for beams subjected to loading in case of isotropic materials:

$$\delta\left(y\right) = \frac{f_1\left(y\right)}{E.I} + \frac{f_2\left(y\right)}{k.A.G}\tag{1}$$

where $\delta\left(y\right)$ represents beam deflection function, E represents elastic modulus, G represents shear modulus, A represents cross-sectional area, E represents E represents shear coefficient, E represents loading and boundary condition functions respectively. Since the PGFRP composite cross-arm is a thin-walled, anisotropic beam, the variations are done by substituting E for shear modulus and E for flexural modulus in the above equation. Equation (2) assesses the maximum deflection in a 3-PB loaded beam, taking into account the cross-arm member's shear deflection.

$$\delta_{max} = \frac{P.L_s^3}{48.E_c.I} + \frac{P.L_s}{4.G_c.A} \tag{2}$$

where, δ_{max} represents maximum deflection and L_s represents the span length. In order to obtain the apparent elastic flexural modulus (E_a) , the effect of shear deformation is neglected resulting in Eq. (3).

$$\delta_{max} = \frac{P.L_s^3}{48.E_a.I} \tag{3}$$

The elastic modulus ratio (E_a/E_c) to the slenderness ratio (L/r) shows that shear deflection effects increase in importance as the direct and inverse proportionality with respect to anisotropy ratio and the slenderness ratio respectively⁷⁹. The effects of shear deflection are most noticeable for L/r ratios below 60^{31} . However, for the

current PGFRP composite cross-arm under study the L/r ratio is found to be 113.54, hence the effect due to shear deformation can be neglected 80,81 . The investigation examines a simply supported beam with a centrally applied load, measuring its deflection.

Flexural creep experiment

The flexural creep test under 3-PB conditions was performed on both the virgin and sleeve reinforced PGFRP composite cross-arms for a span length of 2000 mm, 2500 mm and 3000 mm as per the methodology followed in the previous research³¹. The creep test was carried out for as per ASTM D2990 standards for 1000 h in real-time tropical environmental conditions, with the applied load set as previously established. As seen in Fig. 4, a constant static load was suspended to conduct the creep test. Data on creep strain and mid-span creep deflection were logged and plotted over time. Following that, the relative methodology as a function of time was used to evaluate the effective elastic moduli⁷⁸.

Equation (4) was then used to define the time-dependent reduction factor, $\chi(t)$, for the derived elastic moduli⁴². Equation (5) uses Findley's power law to define the apparent elastic modulus (E_a) over time which helps to arrive at Eq. (6). Time (t), initial elastic modulus (E_0) , elastic creep modulus (E_t) , and a stress-independent constant (n) are all taken into account. For a maximum of 50 years, this equation aids in forecasting the time-dependent behaviour of a full-scale single member PGFRP composite cross-arm with and without the reinforced sleeve structure.

$$\chi(t) = \left(1 + \frac{E_0}{E_t} \cdot t^n\right)^{-1} \tag{4}$$

$$E_a(t) = E_0 \cdot \chi(t) \tag{5}$$

$$E_a(t) = E_0. \left[\frac{1}{1 + \left[\frac{E_0}{E_t} . t^n \right]} \right]$$
 (6)

The long-term resilience of a material is expressed in terms of strain per unit stress using a measurement known as creep compliance. It can be understood as a mathematical equation that can be found with the help of Eq. (7).

$$J(t) = \epsilon(t) / \sigma_0 \tag{7}$$

where σ_0 denotes constant stress applied in MPa, $\sigma(t)$ represents strain that varies with time, and J(t) indicates creep compliance in MPa⁻¹.

Empirical creep model

The Burger model is a physical numerical models to validate creep data. This model incorporates elastic and viscoelastic moduli to predict material behaviour under steady-state creep solution. The Burger model consists of three key components: a linear elastic spring, a dash-pot, and the Kelvin-Voight element (which combines dash-pots and springs) solutions. These components explain creep behaviour through elastic strain, permanent strain, and viscoelastic strain. Typically, tension applied at the displacement tip causes an immediate strain. However, the Burger model has been found unsuitable for predicting the service life of composite materials due to its assumption of a linear relationship between time and material viscosity. Additionally, the model inaccurately predicts a steady decrease in the creep rate over time, assuming a constant relationship rather than one that is dependent on changing variables solve.

Another numerical model used for creep studies is the Norton-Bailey model, which evaluates primary and secondary creep under constant stress and temperature over a specified time period⁸⁸. While this model is effective for analyzing transient creep through steady-state creep responses, it is not well-suited for long-duration predictions^{89,90}. Additionally, the model's applicability is limited to controlled experimental conditions with stable temperatures, which conflicts with the real-time working conditions used in the current study. Experiments on composite specimens have shown that, over extended periods, the data shifts from a positive to a negative fit, highlighting the model's limitations in such scenarios⁸⁶.

The empirical numerical model known as the Findley model addresses the limitations of the previously discussed models. It is particularly effective for predicting long-term creep responses based on early creep strain data⁹¹. The parameters of the Findley model are derived from actual engineering parameters, without being constrained by physical conditions, making it suitable for validating creep responses in the current study. Unlike other models, the Findley model accounts for the influence of physical conditions in the experimental responses, as it evaluates integrated outcomes rather than relying on independent parameters or imposed constraints.

In this investigation, Findley's power law model employing non-linear regression analysis was applied to the material constant and stress component provided empirical support and explanation for transient creep³³. Therefore, the creep pattern simulated using the Findley model is represented by Eq. (8) ⁹²:

$$\varepsilon\left(t\right) = \varepsilon_0 + mt^n \tag{8}$$

where, m and n are the load constant and specific material exponent, respectively, derived from the fitting of the experimental data curve, and ε_0 is the immediate strain following the applied load. The following Eq. (9) is obtained by replacing the elastic strain with the applied constant stress, σ_0 , and dividing it by the initial modulus of elasticity, E_0 :

Total length (mm)	Span lengths (mm)	Breadth (mm)	Width (mm)	Wall thickness (mm)	Moment of inertia (mm ⁴)	Induced load (N)
3651	1000; 1500; 2000; 2500; 3000	102	102	7.8	4.3765×10^{6}	1560

Table 4. Parameters of PGFRP composite cross-arm.

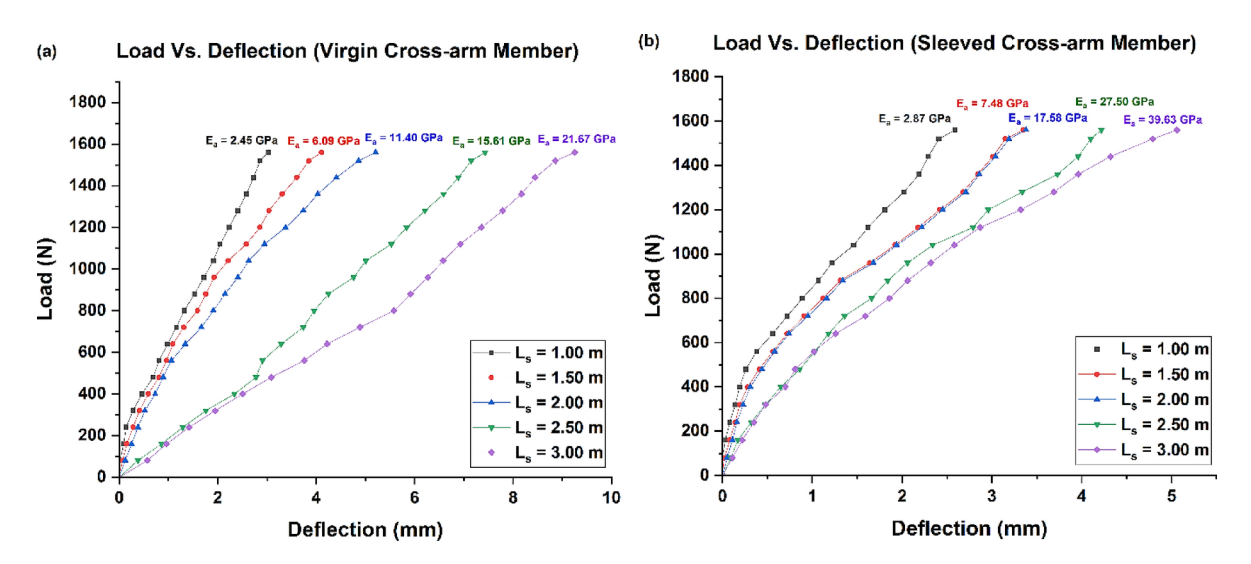


Fig. 5. Load-deflection response of (a) virgin (b) sleeve reinforced PGFRP composite cross-arm member of varying span lengths.

Cross-arm	Max. load induced (N)	Span length (mm)	Deflection (mm)	Apparent elastic modulus (GPa)
		1000	3.03	2.45
		1500	4.11	6.09
Virgin	1560	2000	5.21	11.40
		2500	7.43	15.61
		3000	9.25	21.67
	1560	1000	2.59	2.87
		1500	3.35	7.48
Sleeved		2000	3.38	17.58
		2500	4.22	27.50
		3000	5.06	39.63

Table 5. Summary of outcomes from load-deflection experiment.

$$\varepsilon\left(t\right) = \frac{\sigma_0}{E_0} + mt^n \tag{9}$$

Results and discussions Flexural load-deflection behaviour

In this section, the instantaneous deflection due to induced loads upon the cross-arms against their varying span lengths are explored. To calculate the average value, each measurement was performed five times. The maximum flexural load corresponding to about twice the actual working load of 1560 N was induced to observe the deflection response, which are well within their elastic limits³¹. Table 4 displays the geometric and derived parameters of the PGFRP composite cross-arm under investigation.

Figure 5 illustrates the flexural load–deflection response obtained for both the virgin and sleeve reinforced cross-arm for varying span lengths. The PGFRP composite cross-arm's deflection behaviour and the load applied to it were precisely proportionate and consistent with earlier research, as seen in Fig. 5. This association held true as long as the beam material did not yield and there was little variation 93,94 . The apparent elastic modulus (E_a) was obtained using the Eq. (3) for all the defined sets. The deflection produced upon the cross-arm for the same load increased with the increase in the span length. Table 5 provides a detailed overview of outcomes from this study.

From the Table 5, it can be observed that the enhancement due to the sleeve installation has increased by 14.52%, 18.49%, 35.12%, 43.20% and 45.30% for the span lengths of 1000 mm, 1500 mm, 2000 mm, 2500 mm and 3000 mm respectively whose relationship is consistent with the previous research^{31,44,46}. The improvement in properties is noticeably lower for span lengths of 1000 mm and 1500 mm compared to other spans. This occurs because the inherent rigidity of the cross-arm material resists deformation in shorter spans, while the effect becomes more significant as the deformable region under loading expands. This mechanical capability of the material results in negligible strengthening effect of the sleeve reinforcement. Hence, for the further creep studies the span lengths of 2000 mm, 2500 mm and 3000 mm are considered to further unravel their behaviour to constant static loading.

The PGFRP composite cross-arm is made of unsaturated polyester composites reinforced with pultruded E-glass fibre, which shows good stress characteristics under applied load. Given that glass fibre has a high strength and strength-to-weight ratio, this occurrence resulted from the fibre breaking gradually when the flexural load was applied⁹⁵. When the UPE resin's molecular chain gradually slid and expanded at a high elastic rate, the glass fibre broke more slowly⁹⁶. Similar responses were observed in partially bonded steel-FRP composite bars in terms of load–deflection response⁹⁷. These factors make the utilization of sleeve ideal for applications in the oil, gas, and renewable energy industries, wherein retrofitting is employed to reinforce pipelines, support structures, and offshore platforms that are subjected to challenging environmental conditions⁹⁸.

The pultrusion a UPE matrix reinforced with glass fibre stacked alternately resists the shear strain brought on by the cable's torsional loading^{96,99}. These results were caused by a lamination sequence that had a higher concentration of continuous roving throughout the profile production process^{100,101}. The pultruded composite's exterior layers on both sides led to the load line along the ply orientation¹⁰². Under these conditions, the PGFRP composite cross-arm would be exposed in an orthogonal form, increasing the structure's bending strength¹⁰³. This would shield the composite laminate by preventing the glass fibre from shattering under pressure. Furthermore, the UPE matrix's macromolecular chain stretched and slid more quickly, delaying the rupture of the glass fibre^{104,105}. Furthermore, UPE resin and E-glass fibre complement each other nicely. From a microscopic perspective, the reinforcing fibres stop cracks from spreading by forming covalent chemical bonds with the polymer matrix¹⁰⁶.

Flexural creep behaviour

The flexural creep characteristics of the full-scale virgin and sleeve reinforced PGFRP composite cross-arms were conducted using the 3-PB test as per ASTM D2990 standards. Based on the load–deflection response, these structures allow significant deformation depending on the applied load, accurately reflecting real-world assembly conditions in practical applications. To get the average data, three repetitions of observations were made for each of the said span lengths. According to the literature, a static load level of roughly 1326 N, 1.7 times the load required for each individual cross-arm component to deflect similarly to the assembled cross-arm under working load application, was hung at the middle of the beam³¹. The initial creep deflection was found to be 4.24 mm, 6.83 mm and 8.38 mm for virgin cross-arm and 2.98 mm, 3.91 mm and 4.12 mm for sleeve reinforced cross-arm for the span lengths of 2000 mm, 2500 mm and 3000 mm respectively. As seen in Fig. 6, the testing period lasts for 1000 h in an open tropical environment whose dial gauge values were recorded at intervals of 0, 0.01, 0.1, 0.2, 0.5, 1, 2, 5, 20, 50, 100, 200, 500, 700, and 1000 h, with average temperature of 29.19 °C and average relative humidity of 69.83%.

As a function of time, Fig. 7 displays the average creep strain value resulting from the mid-span deflection findings for three samples with varying span lengths. Under the applied loads, the graph showed a linear relationship between initial creep strain and span length. Additionally, the viscoelastic response of the cross-arm

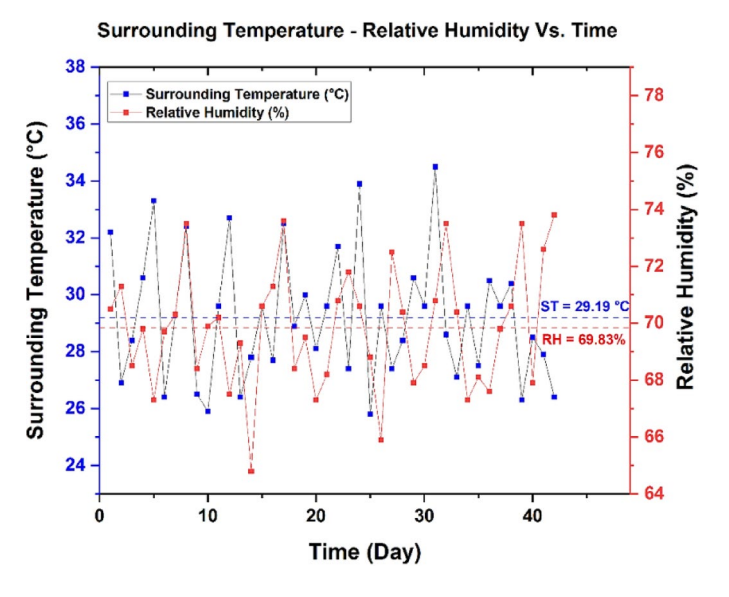


Fig. 6. Relative humidity and temperature data of tropical environment.

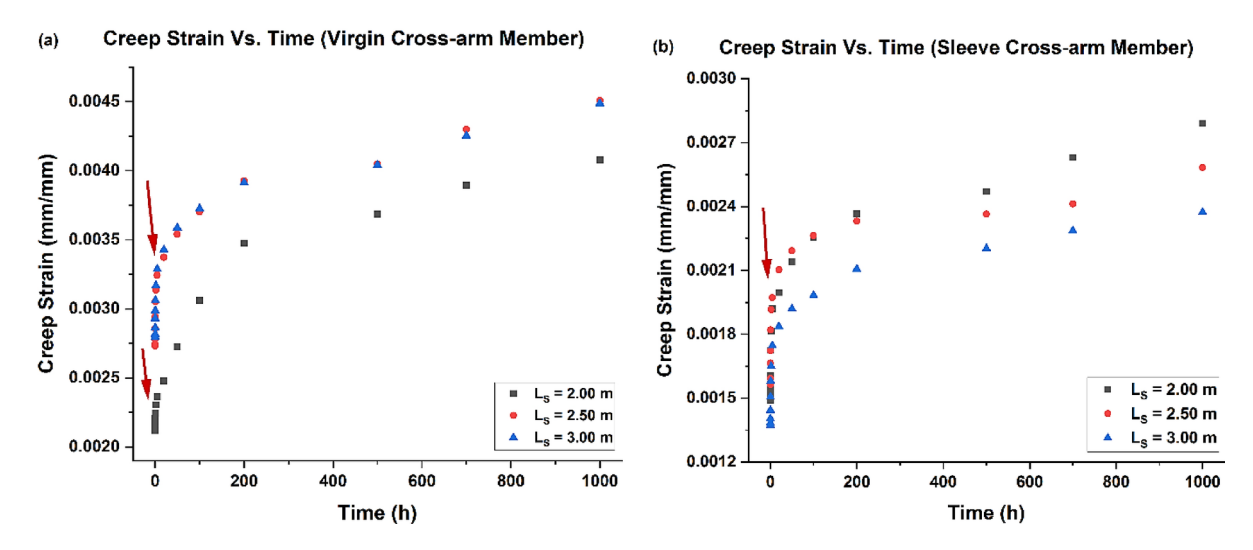


Fig. 7. Creep strain rate graphs of (a) virgin (b) sleeve reinforced cross-arm member.

	Creep strain at the end of the testing period $[\times10^{-3}]$ (mm/mm) at L_S					
Cross-arm	L _S = 2000 mm	L _S = 2000 mm L _S = 2500 mm L _S = 3000 mm				
Virgin	4.08	4.50	4.48			
Sleeved	2.80	2.58	2.37			
Reduction (%)	31.37	42.67	47.10			

Table 6. Creep strain response of virgin and sleeve reinforced PGFRP composite cross-arm.

section remained consistent. This study's creep strain rate demonstrates that while the deformation increases rapidly and decreases over time at the primary stage, it remains consistent in the secondary creep stage as represented by the arrows indicating the transition from the elastic to a constant viscoelastic condition. In contrast to the deformation rate difference between the span lengths of 2000 mm and 2500 mm, the difference between the span lengths of 2500 mm and 3000 mm is observed to be minimal. The reduced characteristics could be attributed to the symmetrical geometry of cross-arm wherein physically the 3000 mm span length was close to the full-scale cross-arm's fixtures in an assembled structure to the transmission tower application. Similar results were observed in thin-walled aluminum tubes reinforced with carbon fiber-reinforced polymer, which has been shown to improve their resistance to lateral crushing, thereby increasing their ability to absorb higher impact energies¹⁰⁷. The alternating creep which corresponds to localized fatigue behaviour as found in railway and highway infrastructure, sleeve retrofitting strengthens beams, columns, and supports to improve load distribution and durability¹⁰⁸.

As can be seen from the graph above, the creep strain in the case of the sleeve-reinforced cross-arm was inversely correlated with the span length. Comparing this study to earlier research, the creep strain impact was similar³¹. The shift in creep strain-span length proportionality can be attributed to the free and constrained anisotropy of the material respectively, especially in the region of high stress susceptible to initiation of fracture. Anisotropic materials, such as polymeric composites, usually show elasticity at first, then viscoelastic behaviour, and finally the plastic deformation stage⁸¹. However, the addition of structural reinforcement fosters a much stronger viscoelastic region due to the enhanced durability and structural rigidity of the overall structure. Table 6 summarizes the creep strain obtained for cross-arm members.

The observed outcome is significant since it demonstrates the cross-arm's ability to tolerate and sustain the loading circumstances⁷⁸. Every aspect of this experimental setup was carefully designed to closely resemble the real-world application. It was discovered that plug-in type sleeve reinforcement could greatly increase the structural integrity and creep resistance of the assembly cross-arm structure in comparison to previous studies^{44,68}. The sleeved cross-arm exhibited lower creep strain than the virgin cross-arm due to the fabric interlayer contact mechanism, which reinforced the outermost layer and significantly reduced slip potential⁹⁴. All things considered, using insulated sleeve reinforcement improved the load-bearing durability and decreased deformation. Table 7 provides the elastic moduli properties based on the observed instantaneous strain values for the constant stress induced by the suspended load.

The increase in creep compliance in virgin cross-arm may have been caused by the structural degradation of the constituents since the cross-arms were exposed to continuously shifting weather conditions throughout the day^{109,110}. Fibre pull-off may result from micro cracks that propagate between the fibres as a result of the increasing stress magnitude¹¹¹. The sleeved PGFRP composite cross-arms exhibited less primary creep due to their higher bending strength compared to the virgin counterparts. Structurally enhanced PGFRP composite

Cross-arm	Span length (mm)	σ ₀ (MPa)	$\varepsilon_0^{}$ (× 10 ⁻³)	$E_{e,0} = \sigma_0 / \varepsilon_0 \text{ (GPa)}$
	2000	7.23	2.120	3.41
Virgin	2500	9.04	2.732	3.31
	3000	10.84	2.793	3.88
	2000	7.23	1.490	4.85
Sleeved	2500	9.04	1.564	5.78
	3000	10.84	1.373	7.90

Table 7. Initial experimental parameters for virgin and sleeved cross-arm members.

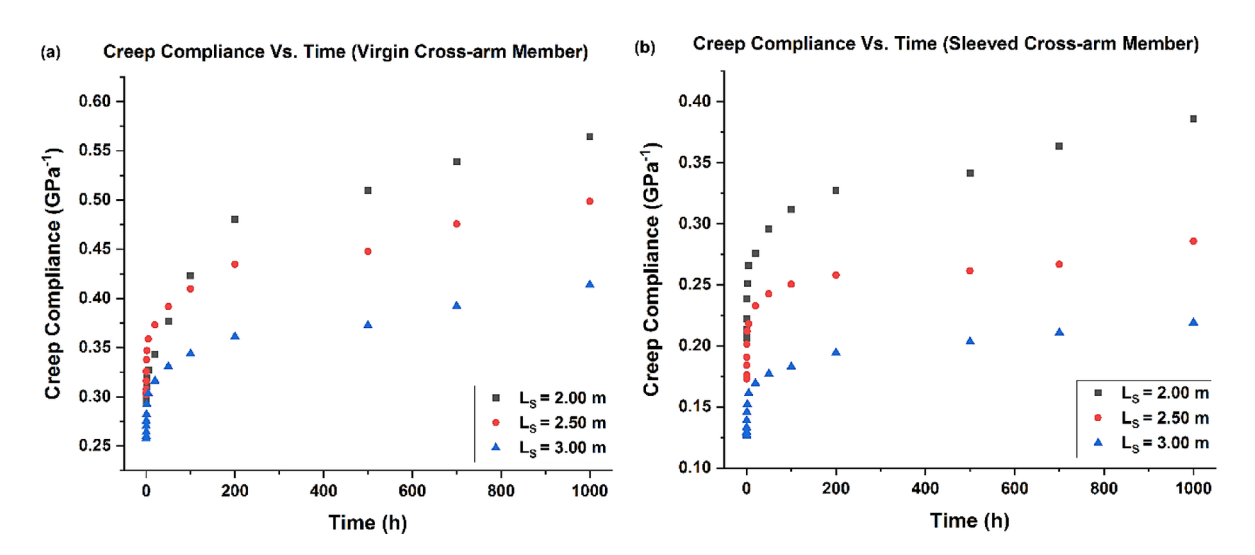


Fig. 8. Creep compliance of virgin and sleeve reinforced cross-arm member.

cross-arms effectively reduced the creep rate, extending the material's service life and maintaining a steady load for longer periods. The creep compliance graphs, as calculated by Eq. (7), are displayed in Fig. 8. Moreover, the findings of this research could be expanded to examine the impact of sleeve reinforcement on localized loading points, sub-surface deformation, energy absorption characteristics, and thin plate buckling behaviour¹¹². These creep compliance factors indicate the improved resilience of the structures which find potential applications in construction and infrastructure, sleeve retrofitting is used to strengthen bridges, buildings, tunnels, and dams, improving their load-bearing capacity and helping prevent structural failures¹¹³.

For the unreinforced (control) specimens, the creep strain exhibited a typical three-phase behavior commonly observed in polymeric composites: an initial primary creep phase with a rapidly decreasing strain rate, followed by a more gradual secondary creep phase characterized by a near-linear strain-time relationship. During the end of testing period, especially under relatively higher stress levels, there existed signs of the tertiary phase, marked by an accelerated increase in strain, were also observed, suggesting progressive damage accumulation and the onset of long-term mechanical instability. In contrast, the sleeve-reinforced specimens demonstrated a noticeably attenuated creep response. The initial strain in these samples was lower due to the increased stiffness introduced by the sleeve layer, and the subsequent strain development occurred at a much slower rate. The secondary phase in reinforced specimens remained linear but flatter in slope, indicating better resistance to time-dependent deformation. No evidence of tertiary creep was observed within the duration of the testing period for the reinforced samples, suggesting that the reinforcement effectively delayed or prevented the onset of long-term degradation mechanisms. Overall, the trend analysis indicated that while both sample types experienced some degree of creep under constant loading, the reinforced specimens showed significantly improved dimensional stability and creep resistance. This trend underscores the role of external reinforcement in limiting matrix deformation, enhancing fibre-matrix interaction, and promoting stress redistribution, all of which contribute to extending the structural integrity of GFRP components in long-duration applications.

Empirical creep model

The study pertaining to the prediction of the cross-arm member's time-dependent full-scale properties is presented in this part. Equation (6), which was derived from general Findley's equation, was utilized to forecast the apparent flexural modulus with time, $E_a(t)$, for the PGFRP composite cross-arm. Table 8 provides a summary of every parameter derived from the experimental data curve fitting. Empirical modeling over extended time periods determined the associated effective moduli using the same deformation method applied to estimate the time-dependent apparent modulus of the full-scale cross-arm member.

Cross-arm	Span length (mm)	ε_0^{-3}	m (10 ⁻⁴)	n	$E_0 = \sigma/\epsilon_0 \text{ (GPa)}$	$E_t = \sigma/m \text{ (GPa)}$	E _t /E ₀	Adj. R ²
	2000	2.070	2.6454	0.2338	3.49	27.33	7.83	0.9865
Virgin	2500	2.670	3.6957	0.2367	3.39	24.48	7.22	0.9883
Viigiii	3000	2.740	3.6990	0.2459	3.96	29.31	7.40	0.9892
	Average	2.493	3.3467	0.2388	3.61	27.04	7.48	0.9880
	2000	1.440	0.9619	0.2179	5.02	75.16	14.97	0.9802
Sleeved	2500	1.527	0.5486	0.1694	5.92	164.78	27.83	0.9846
Sleeved	3000	1.310	0.3664	0.1992	8.27	295.85	35.77	0.9821
	Average	1.426	0.4923	0.1995	6.40	178.60	26.19	0.9823

Table 8. Summary of parameters obtained and derived from Findley Power Law Model.

The equation accurately depicts the observed data, demonstrating the efficacy of Findley's power law in modelling the creep behaviour of the PGFRP composite cross-arm. The study does, however, also show that the generalized Findley's equation produced by this method would not be able to sufficiently characterize strain as the differences between expected and experimental results increase under more stressful circumstances. The general equation for the expected full-scale apparent elastic modulus of the virgin and sleeve-reinforced PGFRP composite cross-arms, respectively, is produced by averaging the values from Table 8 derived from numerical modelling in accordance with the literature³¹ and is shown in Eq. (10) and Eq. (11).

$$E_{a(virgin)}(t) = (3.61) \cdot \left[\frac{1}{1 + \left[\frac{t^{(0.2388)}}{7.48} \right]} \right]$$
 (10)

$$E_{a(sleeved)}(t) = (6.40) \cdot \left[\frac{1}{1 + \left[\frac{t^{(0.1995)}}{26.19} \right]} \right]$$
 (11)

With the obtained average values of 1.426×10^{-4} mm/mm and 2.493×10^{-4} mm/mm, respectively over the varying span lengths, since they are within their elastic limits, the upgraded cross-arm's initial creep strain (ε_0) was lower than that of the existing cross-arm because of the reduced initial creep deflection. In addition, at the conclusion of the test period, the average initial elastic moduli for the sleeved and virgin cross-arms upon varying span lengths within their linear elastic limits were 6.40 GPa and 3.61 GPa respectively. The data exhibit a little discrepancy from the load–deflection test results, which is likely to be caused by variations in the actual weather conditions, such as humidity and temperature, imposing minor deviations in recorded deflections. The strengthened fibre bundles inside the beam, the sleeve structure, and the compliant matrix must all share the applied force, so the enhanced cross-arm will boost the beam's bending strength 114.

In addition, the cross-arm member's viscoelastic reaction appeared to be constant. According to the test's creep deflection rate, the deformation begins quickly in the primary stage and slows down over time, however as previously said, the deflection becomes more uniform in the secondary stage. This study also demonstrates that adding a sleeve construction to the PGFRP composite cross-arm can increase its lifespan by reducing creep strain by about 42.80%. Additionally, as shown by the application of Findley's graph fitting, the measured data validated the power law's capacity to replicate the creep behaviour of the upgraded and current composite cross-arms. The experimental values in the range of 0.9802–0.9892 for the present and increased composite cross-arms, respectively, were well-fitted by the *Adj. R*² for both of the generated graphs and better than the previous research³¹.

Although, averaging of properties and parameters obtained for varying span lengths are done to give a brief overview of the results, as the overall output is linear pertaining to loading within elastic limits, focusing upon the specific span length throws light over other concepts. Comparing the results obtained for the specific span lengths between the cross-arms, it can be seen that (E_t/E_0) is higher for the smallest span length of 2000 mm and for the largest span length of 3000 mm respectively. It is evident that as the span length increases the durability of the material to resist deflections decreases. However, despite this phenomenon, the corresponding span length between the sleeve reinforced cross-arm shows significant enhancement. Numerically, the enhancement in (E_t/E_0) ratio due to the installation of plug-in type sleeve reinforcement increased by 47.70%, 74.10% and 79.31% for the span lengths of 2000 mm, 2500 mm and 3000 mm respectively. This ratio values are important as it determines yet another prominent parameter, namely the reduction factor, which is decisive in life span prediction as it weighs the capability of the cross-arm to resist transient creep when induced to constant static loading for longer durations.

The flexural modulus is influenced by the characteristics of structurally fastened members. Therefore, incorporating the plug-in type sleeve structure is expected to enhance both the flexural modulus and strength. A symmetrically mounted sleeve, secured along its flanges, fully encloses the cross-arm's surfaces, reinforcing areas vulnerable to rupture. This causes the generation of better results as compared to the previous proposed solution³¹. An effective construction for withstanding bending and buckling stresses is created when the fastened flanges act like the web, increasing the moment of inertia with little increase in weight¹¹⁵. This behavior likely

	Initial elastic modulus, E _{e,0} (GPa)		
	Span l	ength (mm)
Cross-arm	2000	2500	3000
Experimental (virgin)	3.41	3.31	3.88
Findley model (virgin)	3.49	3.39	3.96
Error (%)	2.34	2.41	2.06
Experimental (sleeved)	4.85	5.78	7.90
Findley model (sleeved)	5.02	5.92	8.27
Error (%)	3.50	2.42	4.68

Table 9. Comparison of initial elastic modulus between experimental and Findley model.

Precision level	Error range (%)
Excellent	0.1-9.9
Very good	10.0-14.9
Good	15.0-19.9
Above average	20-24.9
Not acceptable	>25.0

Table 10. Precision levels based on percentage errors^{116–118}.

explains why the enhanced cross-arm with sleeve structure configurations surpassed the existing cross-arm sample in flexural modulus values.

In addition, the mechanical sleeve fastening lowers the slip potential ¹¹⁶. Since the shear and flexural strengths are related, strong assembly is necessary to increase flexural strengths ¹¹¹. Therefore, the cross-arm with sleeve structure reinforcement has higher elastic modulus values and less creep strain behaviour than the cross-arm without any improvements. This helps to extend the functional life of the cross-arms used in transmission tower applications.

The long-term deformation behaviour revealed clear distinctions between the control specimens (unreinforced pultruded GFRP) and the sleeve-reinforced specimens. Under sustained loading conditions, the control specimens exhibited a more pronounced time-dependent deformation, characterized by higher creep strain accumulation and earlier onset of nonlinear viscoelastic response. This behaviour is attributed primarily to the intrinsic limitations of the pultruded GFRP matrix, which is more susceptible to microcracking, matrix softening, and fibre-matrix debonding over extended periods of stress exposure. In contrast, the sleeve-reinforced specimens demonstrated significantly improved dimensional stability and resistance to creep deformation. The presence of the sleeve reinforcement acted as a mechanical constraint, effectively redistributing the stress and delaying the onset of matrix degradation. Moreover, the enhanced interfacial bonding between the sleeve and the pultruded substrate contributed to reducing localized stress concentrations and suppressing mechanisms such as interlaminar shear and transverse matrix cracking, which are typically precursors to accelerated creep deformation. Quantitatively, the reinforced specimens maintained a lower rate of strain over time and exhibited a more stable deformation profile across the duration of the long-term loading tests. This difference highlights the effectiveness of the sleeve reinforcement not only in improving immediate load-bearing capacity but also in enhancing the durability and service life of the composite structure under prolonged mechanical stress. The comparative findings underscore the value of sleeve integration as a viable strategy to mitigate time-dependent $failures in GFRP \ structural \ members, particularly in applications \ where \ sustained \ loads \ are \ expected \ to \ dominate$ the service conditions.

Creep model validation

Creep behaviour was confirmed in these investigations by comparing the empirical Findley's model with the initial elastic modulus derived from experimental data. First, it was discovered that the initial modulus of elasticity, or $E_{e,0}$, was inversely proportional to the measured point via the cross-arm members. This comparison, which required determining the initial elastic modulus values for cross-arms by comparing empirical Findley's model with experimental data, is summarized in Table 9. Curiously, the results almost match, indicating that the creep behaviour of the PGFRP composite cross-arm investigation was sufficiently represented by the Findley's power law model. The experimental and empirical model's initial elastic modulus is consistent with previous studies⁸. Table 9 demonstrates that every recorded percentage mistake was less than 5%. This implies that the numerical model (Findley's power law) and the experimental results were exactly in agreement. Using these calculations, the expected elastic modulus value for the cross-arm at the designated time was calculated.

Table 10 displayed the accuracy categories for comparing numerical analysis with experimental results. The provided experimental data stayed near the numerical model and adhered to the guidelines set forth by the

Cross-arm	Span length (mm)	Equation to predict elastic moduli based for cross-arm member
	2000	$E_{e,virgin,2.0m}(t) = 3.49 \times \left(1 + \left(\frac{t^{0.2338}}{7.83}\right)\right)^{-1}$
Virgin	Virgin 2500	$E_{e,virgin,2.5m}(t) = 3.39 \times \left(1 + \left(\frac{t^{0.2367}}{7.22}\right)\right)^{-1}$
	3000	$E_{e,virgin,3.0m}(t) = 3.96 \times \left(1 + \left(\frac{t^{0.2459}}{7.40}\right)\right)^{-1}$
	2000	$E_{e,sleeved,2.0m}(t) = 5.02 \times \left(1 + \left(\frac{t^{0.2179}}{14.97}\right)\right)^{-1}$
Sleeved 2500	2500	$E_{e,sleeved,2.5m}(t) = 5.92 \times \left(1 + \left(\frac{t^{0.1694}}{27.83}\right)\right)^{-1}$
	3000	$E_{e,sleeved,3.0m}(t) = 8.27 \times \left(1 + \left(\frac{t^{0.1992}}{35.77}\right)\right)^{-1}$

Table 11. Prediction of elastic moduli of cross-arm member based on Findley power law.

Cross-arm	Span length (mm)	E _{e,10 years} (GPa)	E _{e,25 years} (GPa)	E _{e,50 years} (GPa)	$\chi_{50 years}$	Adj. R ²
	2000	1.23	1.06	0.95	0.27	0.9888
Virgin	2500	0.11	0.96	0.85	0.25	0.9939
	3000	1.23	1.04	0.92	0.23	0.9906
	2000	2.79	2.54	2.35	0.47	0.9953
Sleeved	2500	4.74	4.59	4.47	0.76	0.9983
	3000	6.51	6.24	6.02	0.73	0.9931

Table 12. Summary of life span prediction based on elastic moduli.

precise numerical model when the percentage error was less than 20%. The creep characteristics of the cross-arms were effectively confirmed by this investigation using accurate and reliable data.

There exists alternate reinforcement methods for the cross-arm application but all those methods have significant drawbacks, which can be easily overcome by the sleeve retrofitting technique. Internal reinforcement using core inserts, can complicate manufacturing and may introduce galvanic corrosion risks if used without adequate insulation. Overwrapping with carbon fibre composites, is more expensive and may raise compatibility concerns due to differences in thermal expansion and stiffness mismatch between the carbon wrap and the glass-based substrate. Hybrid layered laminates, less effective in addressing localized weaknesses or stress concentrations. Bonded FRP plates/strips, the long-term durability of the adhesive interface under environmental exposure remains a critical consideration. Pultrusion with localized reinforcement zones, it may require complex tooling and design adjustments, thereby leading to be expensive. Sleeve reinforcement offers a practical balance between performance improvement, manufacturability, and cost. Unlike bonded plates or inserts, sleeves provide 360-degree confinement, improving shear and torsional performance. Compared to carbon overwraps, sleeves are more cost-effective and compatible with E-glass substrates. While not as integrated as hybrid pultrusion, sleeves offer flexibility for both retrofitting and new installations.

Life span prediction

The full-scale flexural modulus over time, $E_{e,virgin}(t)$ and $E_{e,sleeved}(t)$, for the composite cross-arm whose results are shown in Table 11. Both the virgin and sleeve-reinforced PGFRP composite cross-arms had their modulus reduction factors $(\chi_{e,virgin}(t))$ and $\chi_{e,sleeved}(t)$ assessed over time; the elastic modulus showed the greatest reduction in stiffness during the test period.

As stated earlier, although it is possible find the average of values obtained for different span lengths as expressed by Eq. (10) and Eq. (11), life span prediction based on the independent span lengths provides insights as regards to the total length of cross-arm in real-time applications. This outcome leads to incorporating modifications to cross-arm lengths in suitable places. The length of the current cross-arm is based on the operational feasibility, hence enhancement of its service life for the operational length can be verified and validated by using this approach.

The stiffness decreased most during the early stage, or roughly 24 h into the first test period. However, following the early stage phase, the creep rate reduction fell more slowly due to bending. Furthermore, the graph demonstrates that for both the virgin and sleeved cross-arms, the apparent reduction factor dropped nearly continually. It was determined to forecast the reduction factor and effective moduli over the ensuing 50 years, whose summary is shown in Table 12.

It is evident from the above table that there exists an overall enhancement in service due to the addition of sleeve reinforcement, the most preferable span length corresponds to 2500 mm as it induced the maximum improvement by a factor of 0.51 after 50 years of service. However, in order to minimise discrepancies during the experimental recordings the average values of the varying span lengths are used to generate the predicted life reduction factor as shown in Fig. 9. At the conclusion of the testing period (1000 h), the virgin cross-arm's average elastic moduli were 2.35 GPa. At the same time, the average elastic moduli of the sleeved cross-arm resulted in an effective value of 5.12 GPa. However, it is predicted that the average elastic modulus of the virgin

Life Span Prediction Based on Elastic Modulii

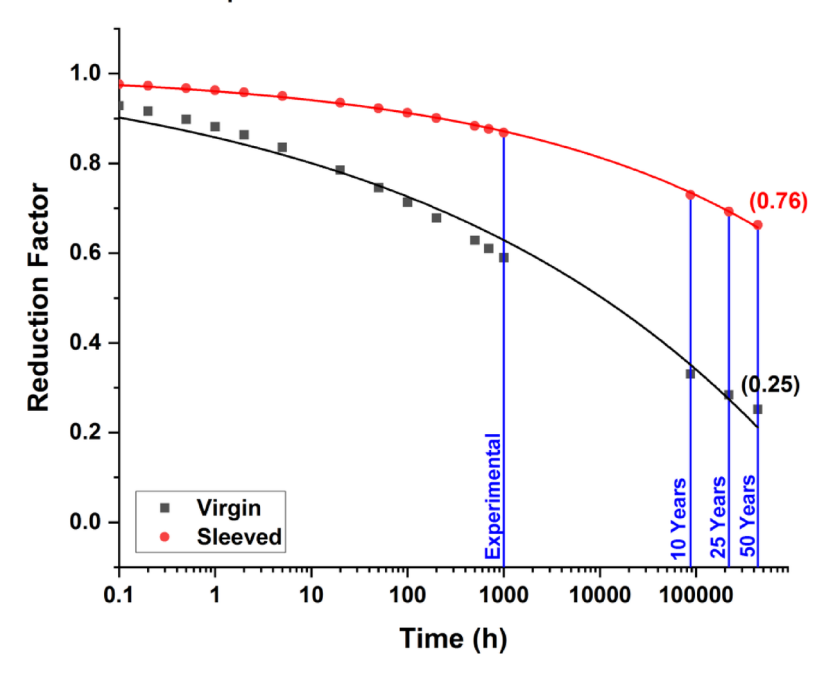


Fig. 9. Life span prediction using reduction factor.

and the sleeved cross-arm member at 50 years will be around 74.79% and 33.75% lower than the average initial modulus, respectively representing an enhancement by about 41%. Consequently, it was discovered that the reduction factor for the PGFRP composite cross-arm was enhanced by about 66% by the use of a plug-in type sleeve construction. It exhibits a pattern that is almost the same as that of the individual cross-arm component and thereby be utilized to predicted the functional service life of the structurally modified cross-arm member.

As shown in Fig. 9, the flexural moduli reductions of the sleeved cross-arm began to progressively decrease throughout the course of the expected period of fifty years in comparison to the virgin cross-arm. When the reduction factor is near 1, the materials usually retain a significant amount of their initial stiffness; however, when the reduction factor is near 0, the structure's stiffness is significantly reduced. Furthermore, as seen in Table 12, the anticipated elastic moduli for the sleeved cross-arm at 10, 25, and 50 years later were still higher than those of the virgin cross-arm and significantly superior to the solution used in the previous work. However, with values around 0.99, which is in line with earlier studies 118,119, the regression analysis—also known as curve fitting—showed the best possible agreement with the actual and anticipated data points for both virgin and sleeved cross-arms.

According to this study, the virgin main member PGFRP composite cross-arms can be strengthened based on the failure mechanism upon the single main member and have their lifespan extended by adding sleeve reinforcement. The cross-arm can be installed on existing transmission towers, without the need for decoupling, because of its simple production, installation, and material availability, which lowers maintenance costs and prolongs the life of the full-scale cross-arm component.

Implementing sleeve-reinforced PGFRP composite cross-arms in transmission towers offers reduced need for frequent repairs and replacements. They have proven to provide higher long-term load bearing properties and higher resistance to electricity as compared to previously utilized materials, making it a cost-effective and safe choice. The material is easily available, easily machinable, possess design flexibility thereby simplifying fabrication, installation and reducing labour costs. Their ease of handling and compatibility with existing tower structures minimize the need for significant modifications, making the installation process more efficient. PGFRP requires minimal maintenance due to its resistance to corrosion and environmental damage whereby they are further protected at the critical region of failure by sleeves that have inherent resistance to environmental factors. This leads to fewer inspections and repairs compared other previously proposed techniques of inclusion of wooden bracing arms or externally affixing honeycomb sandwich structures.

The large-scale adoption of this reinforcement technique for PGFRP cross-arm structures faces a few potential challenges. The initial cost of investment is one such factor, due to procurement and production of sleeve structures. However, in the longer run the return-on-investment will be higher and beneficial. The proposed plug-in type sleeve structures have the capability of direct installation upon the existing cross-arms but it requires precise alignment and torque for desired outcomes. Despite the added cost, sleeve reinforcement significantly improves structural performance, particularly under long-term service conditions. As shown in this study, the reinforced cross-arms exhibited superior resistance to creep deformation, delayed onset of mechanical degradation, and enhanced load-bearing capacity. These improvements directly translate to extended service life and reduced likelihood of in-service failure, critical factors in utility infrastructure such as

transmission and distribution poles. One of the most compelling benefits lies in the reduction of maintenance frequency and replacement costs. Traditional GFRP cross-arms, while corrosion-resistant, can suffer from longterm deformation and fatigue in demanding environments. Reinforced versions are more robust, potentially lowering inspection intervals and minimizing emergency repairs. Over time, the savings in labour, downtime, and material replacement can outweigh the higher initial investment. Sleeve-reinforced GFRP also contributes to improved system reliability and safety. For power distribution networks, failure of a cross-arm can lead to significant operational disruption and public safety hazards. Reinforcement helps mitigate these risks, offering a more resilient design solution, an intangible but critical component of the cost-benefit equation. The more sound observation would be that the incorporation of sleeve retrofits eliminates the catastrophic failures that would generally lead to fatal accidents. While the use of sleeve-reinforced GFRP cross-arms entails a moderate increase in initial cost, the long-term financial and functional advantages, including extended durability, lower maintenance requirements, and improved reliability, make it a cost-effective and strategic investment for infrastructure systems requiring high performance under sustained loading conditions. Despite the above stated shortcomings sleeve reinforced PGFRP composite cross-arms however are much feasible and durable than the previously proposed solution of installation of wooden bracing arms and adhesively bonded honeycomb sandwich panels capable of reducing catastrophic failures and fatal accidents.

Conclusion

This work investigates the elastic properties of a full-scale PGFRP composite cross-arm reinforced with a sleeve structure, thereby filling a substantial research gap in the feasibility of enhancing the cross-arms' structural integrity and longevity in high-rise transmission towers. In order to evaluate the cross-arms' elastic characteristics for creep response and deflection behaviour, this study used a thorough experimental technique with a three-point bending flexural test. The experimental and numerical computation results allow for the following conclusion to be made.

- The study used a comparative analysis to assess the effective flexural modulus of a sleeve reinforced cross-arm members to its virgin counterpart that were loaded throughout a range of span lengths.
- The research demonstrated that its empirical methodology could reproduce the viscoelastic response of the cross-arm by successfully simulating the composite cross-arm creep behaviour using Findley's power law.
- Key findings showed that, in comparison to the current construction, the sleeve reinforced structure maintained superior mechanical properties throughout time and decreased deflection by about 45%.
- According to predictions for up to 50 years of operation, the improved cross-arm with the sleeve structure
 had an elastic modulus reduction of roughly 34% as opposed to roughly 75% for the virgin cross-arm. This
 improvement demonstrated greater bending strength, enhanced creep resistance, less deflection, and possibly
 longer longevity.
- The freedom of design, stress transfer capabilities and resistance to physical conditions of the sleeve structures
 make them an ideal choice for applications such as retrofitting columns in bridges as a primary safety measure
 to avoid catastrophic collapse, in heavy vehicles to reinforce axes to withstand torsional and shear loads, in
 boats to strengthen the wind sail arms to resist dynamic loads and in ships to protect anchors from aquatic
 erosions in addition to enhancing durability.

The results of this study suggest that incorporating a plug-in type sleeve structure could extend the life of the cross-arm in transmission towers and reduce maintenance costs. The potential application of sleeve structures in transmission tower cross-arm design optimization is highlighted by the cross-arm's enhanced mechanical performance, particularly in terms of reduced deflection and greater creep resistance. These findings imply that lifetime and durability could be greatly enhanced in the context of high-voltage transmission infrastructure.

Data availability

The datasets used and/or analysed during the current study available from the corresponding author on reasonable request.

Received: 1 March 2025; Accepted: 30 April 2025

Published online: 08 May 2025

References

- Salleh, N. H. M., Chatri, F. & Huixin, L. Economic and environmental analysis of Malaysia's 2025 renewable and sustainable energy targets in the generation mix. *Heliyon* 10, e30157. https://doi.org/10.1016/j.heliyon.2024.e30157 (2024).
- Asyraf, M. R. M., Ishak, M. R., Sapuan, S. M. & Yidris, N. Conceptual design of creep testing rig for full-scale cross arm using TRIZ-morphological chart-analytic network process technique. J. Mater. Res. Technol. 8, 5647–5658. https://doi.org/10.1016/j.jm rt.2019.09.033 (2019).
- Itam, Z., Ishak, Z. A. M., Yusof, Z. M., Salwi, N. & Zainoodin, M. Effect on the temperature behavior of glass fiber reinforced polymer (GFRP) in various application—A review. In AIP Conference Proceedings vol. 2031 1. https://doi.org/10.1063/1.5066982 (2018).
- 4. Sukumaar, V. N., Ishak, M. R., Na'Im Abdullah, M., Zuhri, M. Y. M. & Rizal, M. A. M. Experimental investigation and theoretical prediction of sleeve reinforced PGFRP composite under flexural loading for cross-arm application. *Results Eng.* 25, 103735. https://doi.org/10.1016/j.rineng.2024.103735 (2025).
- Li, J., Wang, L. & Zhang, S. Lightning protection design for 20 kV insulated crossarm of different altitudes. In *International Conference in Communications, Signal Processing, and Systems* 239–249. https://doi.org/10.1007/978-981-99-2362-5_30 (2022).
- Ali, S. S. S. et al. Critical determinants of household electricity consumption in a rapidly growing city. Sustainability 13, 4441. https://doi.org/10.3390/su13084441 (2021).

- 7. Sukumaar, V. N. et al. Experimental investigation of flexural mechanical and flexural creep properties of sleeved PGFRP composite used in transmission tower application. *Glob. Congr. Manuf. Manag.* https://doi.org/10.1007/978-3-031-80341-3_23 (2023).
- 8. Johari, A. N., Ishak, M. R., Leman, Z., Yusoff, M. Z. M. & Asyraf, M. R. M. Influence of CaCO₃ in pultruded glass fiber/unsaturated polyester resin composite on flexural creep behavior using conventional and time-temperature superposition principle methods. *Polimery* 15, 156. https://doi.org/10.14314/polimery.2020.11.6 (2020).
- Harizi, W. et al. Damage mechanisms assessment of glass fiber-reinforced polymer (GFRP) composites using multivariable analysis methods applied to acoustic emission data. Compos. Struct. 289, 115470. https://doi.org/10.1016/j.compstruct.2022.115470 (2022).
- Mohamad, D. et al. Numerical simulation on the statics deformation study of composite cross arms of different materials and configurations. In IOP Conference Series: Materials Science and Engineering vol. 530 012028. https://doi.org/10.1088/1757-899X/ 530/1/012028 (2019).
- Sukumaar, V. N. et al. Structural sleeve reinforcement upon PGFRP composite cross-arm members for transmission tower application: A comprehensive review on hierarchical development, potential incorporation and future scope. Next Res. https://doi.org/10.1016/j.nexres.2025.100189 (2025).
- 12. Palanisamy, S. et al. Wear properties and post-moisture absorption mechanical behavior of kenaf/banana-fiber-reinforced epoxy composites. Fibers 10, 32. https://doi.org/10.3390/fib10040032 (2022).
- 13. Ahsan, M. et al. Historical review of advancements in insulated cross-arm technology. *Energies* 15, 8221. https://doi.org/10.3390/en15218221 (2022).
- Yamanaka, A., Ishimoto, K. & Tatematsu, A. Direct lightning surge analysis of distribution lines considering LEMPs from lightning channel and struck pole in EMT simulation. *IEEE Trans. Electromagn. Compat.* https://doi.org/10.1109/TEMC.2023.3319032 (2023).
- 15. Khadka, N., Bista, D., Gomes, C., Sharma, S. & Adhikary, B. Distribution network impact assessment with geometrically identified strike points: An approach. In 36th International Conference on Lightning Protection (ICLP) vol. 2022 1–6. https://doi.org/10.110 9/ICLP56858.2022.9942530 (2022).
- 16. Amir, A. L., Ishak, M. R., Yidris, N., Zuhri, M. Y. M. & Asyraf, M. R. M. Potential of honeycomb-filled composite structure in composite cross-arm component: A review on recent progress and its mechanical properties. *Polymers* 13, 1341. https://doi.org/10.3390/polym13081341 (2021).
- 17. Asyraf, M. R. M. et al. Creep properties and analysis of cross arms' materials and structures in latticed transmission towers: Current progress and future perspectives. *Materials* 16, 1747. https://doi.org/10.3390/ma16041747 (2023).
- 18. Abd Halim, S. et al. Lightning back flashover tripping patterns on a 275/132 kV quadruple circuit transmission line in Malaysia. *IET Sci. Meas. Technol.* 10, 344–354. https://doi.org/10.1049/iet-smt.2015.0199 (2016).
- Rajeev, P., Bandara, S., Gad, E. & Shan, J. Structural assessment techniques for in-service crossarms in power distribution networks. *Infrastructures* 7, 94. https://doi.org/10.3390/infrastructures7070094 (2022).
- Alhayek, A. et al. Flexural creep behaviour of pultruded GFRP composites cross-arm: A comparative study on the effects of stacking sequence. *Polymers* 14, 1330. https://doi.org/10.3390/polym14071330 (2022).
- 21. Huangfu, S. E. et al. Web tension field action of a stainless steel section with stiffened web and folded flanges under bending and
- shear interaction. *Sci. Rep.* **15**, 5146. https://doi.org/10.1038/s41598-025-89314-4 (2025).

 22. Betts, D., Sadeghian, P. & Fam, A. Experimental and analytical investigations of the flexural behavior of hollow ±55 filament wound GFRP tubes. *Thin-Walled Struct.* **159**, 107246. https://doi.org/10.1016/j.tws.2020.107246 (2021).
- 23. Kalyani, G. & Pannirselvam, N. Experimental and numerical investigations on RC beams flexurally strengthened utilizing hybrid FRP sheets. *Results Eng.* 19, 101337. https://doi.org/10.1016/j.rineng.2023.101337 (2023).
- 24. Cardoso, D. C. T. & Harries, K. A. A viscoelastic model for time-dependent behavior of pultruded GFRP. Constr. Build. Mater. 208, 63–74. https://doi.org/10.1016/j.conbuildmat.2019.02.155 (2019).
- Nor, S. F. M. et al. Systematic approaches and analyses on voltage uprating of 132 kV transmission lines: A case study in Malaysia. Appl. Sci. 11, 9087. https://doi.org/10.3390/app11199087 (2021).
- Namasivayam Sukumaar, V., Arjunan, S., Pandiaraj, L. N. & Narayanan, A. Experimental investigation of 3D printed polylactic acid and polylactic acid-hydroxyapatite composite through material extrusion technique for biomedical application. J. Thermoplast. Compos. Mater. https://doi.org/10.1177/08927057241255883 (2024).
- 27. Wang, H., Lu, W. & Zhan, W. Dynamic response and damage mechanism of reinforced concrete beam bridges under rockfall impacts. Sci. Rep. 15, 5090. https://doi.org/10.1038/s41598-025-89061-6 (2025).
- 28. Asyraf, M. R. M., Ishak, M. R., Sapuan, S. M. & Yidris, N. Influence of additional bracing arms as reinforcement members in wooden timber cross-arms on their long-term creep responses and properties. *Appl. Sci.* 11, 2061. https://doi.org/10.3390/app11 052061 (2021).
- Asyraf, M. R. M., Ishak, M. R., Sapuan, S. M. & Yidris, N. Utilization of bracing arms as additional reinforcement in pultruded glass fiber-reinforced polymer composite cross-arms: Creep experimental and numerical analyses. *Polymers* 13, 620. https://doi. org/10.3390/polym13040620 (2021).
- Amir, A. L. et al. Full-scale evaluation of creep coefficients and viscoelastic moduli in honeycomb sandwich pultruded GFRP composite cross-arms: Experimental and numerical study. Results Eng. 21, 101850. https://doi.org/10.1016/j.rineng.2024.101850 (2024).
- Amir, A. L., Ishak, M. R., Yidris, N. & Zuhri, M. Y. M. Flexural creep response of honeycomb sandwich pultruded GFRP composite cross-arm: Obtaining full-scale viscoelastic moduli and creep coefficients. J. Mater. Res. Technol. 29, 225–241. https://doi.org/10.1016/j.jmrt.2024.01.091 (2024).
- 32. Amir, A. L., Yamunan, S., Ishak, M. R., Yidris, N. & Zuhri, M. Y. M. Flexural creep behavior in utilization of woven glass-fibre as reinforcement in pultruded glass fibre-reinforced polymer composite cross-arms: Experimental and numerical analysis. In E3S Web of Conferences vol. 477 00007. https://doi.org/10.1051/e3sconf/202447700007 (2024).
- 33. Cui, X., Jiao, Q., Wang, W., Zhang, L. & Lu, Y. Exceptionally strong and ductile bulk metallic glass composite with bioinspired architecture mimicking porcupine fish spine. J. Mater. Sci. Technol. 195, 22–28. https://doi.org/10.1016/j.jmst.2024.01.033 (2024).
- Dicha, H. M., Chaudhary, S., Husain, M. N. & Krishnaraj, R. Banana fibre-reinforced diatomaceous earth slurry treatment of recycled aggregate for enhanced structural concrete performance. Sci. Rep. 15, 4717. https://doi.org/10.1038/s41598-024-8476 2-w (2025).
- 35. Li, X., Liu, W., Fang, H., Huo, R. & Wu, P. Flexural creep behavior and life prediction of GFRP-balsa sandwich beams. *Compos. Struct.* 224, 111009. https://doi.org/10.1016/j.compstruct.2019.111009 (2019).
- 36. Selvaraj, M., Kulkarni, S. & Babu, R. R. Analysis and experimental testing of a built-up composite cross arm in a transmission line tower for mechanical performance. *Compos. Struct.* **96**, 1–7. https://doi.org/10.1016/j.compstruct.2012.10.013 (2013).
- 37. Yankin, A., Perveen, A. & Talamona, D. Investigation and prediction of fatigue performance of SLM 316 L stainless steel based on small build orientation variations and heat treatment effects. *Sci. Rep.* 15, 4583. https://doi.org/10.1038/s41598-025-89003-2 (2025).
- 38. Bell, A. M. et al. UV aged epoxy coatings—Ecotoxicological effects and released compounds. *Water Res. X* 12, 100105. https://doi.org/10.1016/j.wroa.2021.100105 (2021).
- 39. Khotbehsara, M. M. et al. Effect of elevated in-service temperature on the mechanical properties and microstructure of particulate-filled epoxy polymers. *Polym. Degrad. Stab.* 170, 108994. https://doi.org/10.1016/j.polymdegradstab.2019.108994 (2019).

- 40. Kirubakaran, R. et al. Investigation of corrosion and water absorption of biomass natural coir fiber/hBN reinforced epoxy hybrid composites using different optimisation approaches. Sci. Rep. 15, 3388. https://doi.org/10.1038/s41598-025-87673-6 (2025).
- 41. Jalali, E., Soltanizadeh, H., Chen, Y., Xie, Y. M. & Sareh, P. Selective hinge removal strategy for architecting hierarchical auxetic metamaterials. *Commun. Mater.* 3, 97. https://doi.org/10.1038/s43246-022-00322-7 (2022).
- 42. Yassin, M. H., Lakys, R. E., Merouani, Z. E., Jumah, A. & Farhat, M. H. Performance analysis of palm tree microfibers in concrete. Sci. Rep. 15, 5128. https://doi.org/10.1038/s41598-024-84111-x (2025).
- 43. Chen, Y. et al. Multi-stability of the hexagonal origami hypar based on group theory and symmetry breaking. Int. J. Mech. Sci. 247, 108196. https://doi.org/10.1016/j.ijmecsci.2023.108196 (2023).
- Palanisamy, S. et al. Tailoring epoxy composites with Acacia caesia bark fibers: Evaluating the effects of fiber amount and length on material characteristics. Fibers 11, 63. https://doi.org/10.3390/fib11070063 (2023).
- 45. Syamsir, A. et al. Recent advances of GFRP composite cross arms in energy transmission tower: A short review on design improvements and mechanical properties. *Materials* 16, 2778. https://doi.org/10.3390/ma16072778 (2023).
- 46. Asyraf, M. R. M. et al. Filament-wound glass-fibre reinforced polymer composites: Potential applications for cross arm structure in transmission towers. *Polym. Bull.* **80**, 1059–1084. https://doi.org/10.1007/s00289-022-04114-4 (2023).
- 47. Cao, L., Guo, L. & Dhanasekar, M. Development of a new outer sleeve assembly for beam-column connections. *J. Constr. Steel Res.* **164**, 105769. https://doi.org/10.1016/j.jcsr.2019.105769 (2020).
- 48. Liu, Y., Li, X., Zheng, X. & Song, Z. Experimental study on seismic response of precast bridge piers with double-grouted sleeve connections. *Eng. Struct.* 221, 111023. https://doi.org/10.1016/j.engstruct.2020.111023 (2020).
- Lu, X. et al. Hysteretic behavior of composite beam-reinforced concrete column frame. Results Eng. 23, 102549. https://doi.org/1 0.1016/j.rineng.2024.102549 (2024).
- 50. Wang, P., Liu, P. & Ao, W. Study on the nonlinear viscoelastic behavior of rubber composites filled with silica. *Alex. Eng. J.* 97, 1–7. https://doi.org/10.1016/j.aej.2024.03.081 (2024).
- 51. Higgoda, T. M., Elchalakani, M., Kimiaei, M. & Guo, X. Flexural behaviour of bolted flange-plate with bonded sleeve splice connections for pultruded GFRP circular tubular hollow beams. Structures 63, 106312. https://doi.org/10.1016/j.istruc.2024.106
- 52. Palanisamy, S. et al. Characterization of *Acacia caesia* bark fibers (ACBFs). *J. Nat. Fibers* 19, 10241–10252. https://doi.org/10.108 0/15440478.2021.1993493 (2022).
- 53. Lu, Z. et al. Experimental study on flexural behaviour of prefabricated concrete beams with double-grouted sleeves. *Eng. Struct.* 248, 113237. https://doi.org/10.1016/j.engstruct.2021.113237 (2021).
- 54. Azuwa, S. B. & Yahaya, F. B. M. Experimental investigation and finite element analysis of reinforced concrete beams strengthened by fibre reinforced polymer composite materials: A review. *Alex. Eng. J.* **99**, 137–167. https://doi.org/10.1016/j.aej.2024.05.017 (2024)
- 55. Zhao, L., Chen, G. & Huang, C. Experimental investigation on the flexural behavior of concrete reinforced by various types of steel fibers. Front. Mater. 10, 1301647. https://doi.org/10.3389/fmats.2023.1301647 (2023).
- 56. Ou, J., Shao, Y., Huang, C., Chen, Y. & Bi, X. Flexural behavior of circular concrete filled steel tubular members strengthened by CFRP sheets. Structures 55, 201–214. https://doi.org/10.1016/j.engstruct.2024.117610 (2023).
- 57. Palanisamy, S. et al. Mechanical properties of *Phormium tenax*-reinforced natural rubber composites. *Fibers* **9**, 11. https://doi.org/10.3390/fib9020011 (2021).
- 58. Tiutkin, O., Autelitano, F., Giuliani, F. & Neduzha, L. Stress-strain behavior of railway embankments stabilized with grouted micropiles. *Alex. Eng. J.* 102, 75–81. https://doi.org/10.1016/j.aej.2024.05.088 (2024).
- 59. Collini, L., Garziera, R., Corvi, A. & Cantarelli, G. Slip strength of COR-TEN and Zn-coated steel preloaded bolted joints. *Results Eng.* 22, 102009. https://doi.org/10.1016/j.rineng.2024.102009 (2024).
- Sun, Y. et al. Flexural behaviours of pretensioned prestressed concrete-UHDC composite beams reinforced with CFRP bars. Compos. Struct. 322, 117385. https://doi.org/10.14006/j.jzjgxb.2020.S1.019 (2023).
- 61. Qiu, M., Shao, X., Zhu, Y., Hussein, H. H. & Liu, Y. Tensile and flexural tests on ultrahigh performance concrete grouted sleeve connection. *Struct. Concr.* 24, 703–720. https://doi.org/10.1016/j.compstruct.2008.05.016 (2023).
- 62. Zamzam, O., Ramzy, A. A., Abdelaziz, M., Elnady, T. & El-Wahab, A. A. A. Structural performance evaluation of electric vehicle chassis under static and dynamic loads. Sci. Rep. 15, 5168. https://doi.org/10.1038/s41598-025-86924-w (2025).
- 63. Gribniak, V. et al. Quantifying the flexural stiffness changes in the concrete beams with externally bonded carbon fiber sheets under elevated environment temperature. *Alex. Eng. J.* 104, 688–700. https://doi.org/10.1016/j.aej.2024.08.044 (2024).
- 64. Senthilkumar, K. et al. Dual cantilever creep and recovery behavior of sisal/hemp fibre reinforced hybrid biocomposites: Effects of layering sequence, accelerated weathering and temperature. *J. Ind. Text.* 51(2), 2372S-2390S. https://doi.org/10.1177/1528083
- Du, J., Feng, Y., Liu, G., Liao, X. & Zhang, F. Strong yet ductile bionic steel by mitigating local stress concentration function. J. Mater. Sci. Technol. 192, 190–200. https://doi.org/10.1016/j.jmst.2023.12.066 (2024).
- 66. Fode, T. A. et al. Effects of different lengths and doses of raw and treated sisal fibers in the cement composite material. *Sci. Rep.* 15, 1603. https://doi.org/10.1038/s41598-025-86046-3 (2025).
- 67. Karthik, A. et al. A review on surface modification of plant fibers for enhancing properties of biocomposites. *Chem. Select* **9**, e202400650. https://doi.org/10.1002/slct.202400650 (2024).
- Latif, A. A. et al. Experimental and numerical analysis of pGFRP and wood cross-arm in latticed tower: A comprehensive study of mechanical deformation and flexural creep. Sci. Rep. 15, 1432. https://doi.org/10.1038/s41598-024-83634-7 (2025).
- 69. Fan, Q., Duan, H. & Xing, X. A review of composite materials for enhancing support, flexibility and strength in exercise. *Alex. Eng. J.* 94, 90–103. https://doi.org/10.1016/j.aej.2024.03.048 (2024).
- Islami, D. P. et al. Structural design parameters of laminated composites for marine applications: Milestone study and extended review on current technology and engineering. Results Eng. 24, 103195. https://doi.org/10.1016/j.rineng.2024.103195 (2024).
- 71. Li, Y. et al. Micro and macro experimental study of using the new cement-based self-stress grouting material to solve shrinkage problem. J. Mater. Res. Technol. 17, 3118–3137. https://doi.org/10.1016/j.jmrt.2022.01.148 (2022).
- Li, W. W. et al. Study on shear performance of discontinuous PBL connectors with double holes. Alex. Eng. J. 88, 45–57. https://doi.org/10.1016/j.aej.2024.01.006 (2024).
- Sajid, Z., Karuppanan, S., Sallih, N., Kee, K. E. & Shah, S. Z. H. Role of washer size in mitigating adverse effects of bolt-hole clearance in a single-lap, single-bolt basalt composite joint. *Compos. Struct.* 266, 113802. https://doi.org/10.1016/j.compstruct.2021.113802 (2021).
- Hao, G. O. N. G., Jianhua, L. I. U. & Huihua, F. E. N. G. Review on anti-loosening methods for threaded fasteners. Chin. J. Aeronaut. 35, 47–61. https://doi.org/10.1016/j.cja.2020.12.038 (2022).
- 75. Yang, K. et al. Failure analysis and size optimization of CFRP composite single-lap bonded joints based on the influence of multiple parameters. Sci. Rep. 14, 32034. https://doi.org/10.1038/s41598-024-83605-y (2024).
- Gopi Chander, N., Jayaraman, V. & Sriram, V. Comparison of ISO and ASTM standards in determining the flexural strength of denture base resin. Eur. Oral Res. 53, 137–140. https://doi.org/10.26650/eor.20190072 (2019).
- 77. ASTM-D2990 standard test methods for tensile, compressive, and flexural creep and creep-rupture of plastics. In *Annual Book ASTM Standards* vol. 2017, i:1–20.
- 78. Fan, Z. et al. Displacement and stress response of open-web girders under near field explosive loading. *Sci. Rep.* 14, 30782. https://doi.org/10.1038/s41598-024-80915-z (2024).

- 79. Bank, L. C. Properties of pultruded fiber reinforced plastic structural members. *Transp. Res. Rec.* 1223. http://onlinepubs.trb.org/Onlinepubs/trr/1989/1223/1223-014.pdf (1989).
- 80. Abu Bakar, M. S. et al. The reduction factor of pultruded glass fibre-reinforced polyester composite cross-arm: a comparative study on mathematical modelling for life-span prediction. *Materials* 16, 5328. https://doi.org/10.3390/ma16155328 (2023).
- 81. Fahmy, A. S., Swelem, S. M. & Khalifa, K. M. Experimental investigation on an innovative built-up cold-formed steel I-section connection. *Alex. Eng. J.* 107, 698–710. https://doi.org/10.1016/j.aej.2024.09.010 (2024).
- 82. Asyraf, M. R. M., Ishak, M. R., Sapuan, S. M., Yidris, N. & Ilyas, R. A. Woods and composites cantilever beam: A comprehensive review of experimental and numerical creep methodologies. *J. Mater. Res. Technol.* **9**, 6759–6776. https://doi.org/10.1016/j.jmrt. 2020.01.013 (2020).
- 83. Yin, W., Zhao, Z., Lin, H. & Ma, P. Advances in creep behaviors of textile composites. *Appl. Compos. Mater.* **30**, 1949–1978. https://doi.org/10.1007/s10443-023-10154-4 (2023).
- 84. Xu, B., van den Hurk, B., Lugger, S. J., Blok, R. & Teuffel, P. Creep analysis of the flax fiber-reinforced polymer composites based on the time-temperature superposition principle. *Sci. Eng. Compos. Mater.* 30, 20220218. https://doi.org/10.1515/secm-2022-02 18 (2023).
- 85. Asyraf, M. R. M. et al. Creep test rig for cantilever beam: Fundamentals, prospects and present views. J. Mech. Eng. Sci. 14, 6869–6887. https://doi.org/10.15282/jmes.14.2.2020.26.0538 (2020).
- 86. Asyraf, M. R. M., Ishak, M. R., Sapuan, S. M. & Yidris, N. Comparison of static and long-term creep behaviors between balau wood and glass fiber reinforced polymer composite for cross-arm application. *Fibers Polym.* 22, 793–803. https://doi.org/10.1007/s12221-021-0512-1 (2021).
- 87. Ndong Bidzo, C. H., Pambou Nziengui, C. F., Ikogou, S., Kaiser, B. & Moutou Pitti, R. Mechanical properties of glued-laminated timber made up of mixed tropical wood species. *Wood Mater. Sci. Eng.* 17, 809–822. https://doi.org/10.1080/17480272.2021.196 0422 (2022).
- 88. Sattar, M., Othman, A. R., Kamaruddin, S., Azad Alam, M. & Azeem, M. Creep parameters determination by omega model to Norton bailey law by regression analysis for austenitic steel SS-304. *Solid State Phenom.* 324, 188–197. https://doi.org/10.4028/www.scientific.net/SSP.324.188 (2021).
- 89. Asyraf, M. R. M., Ishak, M. R., Razman, M. R. & Chandrasekar, M. Fundamentals of creep, testing methods and development of test rig for the full-scale crossarm: A review. *J. Teknol. (Sci. Eng.)* https://doi.org/10.11113/jt.v81.13402 (2019).
- Katouzian, M., Vlase, S., Marin, M. & Öchsner, A. Creep response of fiber-reinforced composites: A review. Discov. Mech. Eng. 1, 3. https://doi.org/10.1007/s44245-022-00003-2 (2022).
- 91. Amjadi, M. & Fatemi, A. Creep behavior and modeling of high-density polyethylene (HDPE). *Polym. Test.* **94**, 107031. https://doi.org/10.1016/j.polymertesting.2020.107031 (2021).
- 92. Alhayek, A. et al. A mathematical model of flexural-creep behaviour for future service expectancy of a GFRP composite cross-arm with the influence of outdoor temperature. Fibers Polym. 24, 2425–2437. https://doi.org/10.1007/s12221-023-00235-3 (2023).
- 93. Xu, Y., Xu, C., Zhang, C. & Zhang, X. Experimental and numerical study on the mechanical properties of F type socket joints for rectangular pipe jacking with steel screw connection. Sci. Rep. 14, 30952. https://doi.org/10.1038/s41598-024-81974-y (2024).
- 94. Shi, T., Li, Y., Qiu, Y. & Zhu, Y. Design and mechanical properties analysis of a novel CFRP tendons anchorage structure. *Alex. Eng. J.* 109, 591–602. https://doi.org/10.1016/j.aej.2024.09.088 (2024).
- 95. Rohani Nejad, S., Hesari, S. & Mirbagheri, S. M. H. Effect of nickel and copper shells on mechanical properties of advanced lightweight TPU metamaterials during uniaxial compression. *Sci. Rep.* 14, 31131. https://doi.org/10.1038/s41598-024-82317-7 (2024).
- Syamsir, A. et al. Performance analysis of full assembly glass fiber-reinforced polymer composite cross-arm in transmission tower. *Polymers* 14, 1563. https://doi.org/10.3390/polym14081563 (2022).
- 97. Sun, Y. et al. Flexural behavior of concrete beams reinforced by partially unbonded steel-FRP composite bars. Eng. Struct. 272, 115050. https://doi.org/10.1016/j.engstruct.2022.115050 (2022).
- 98. Bakir, D., Savaş, S. & Tuğrul Tunç, E. Improving structural adhesion: experimental and numerical analysis of repair mortar in reinforced concrete. *Appl. Sci.* 15, 1463. https://doi.org/10.3390/app15031463 (2025).
- 99. Hu, Y. et al. Fracture characteristics in micron molybdenum wires under cyclic torsion loading. J. Mater. Sci. Technol. 191, 220–232. https://doi.org/10.1016/j.jmst.2023.12.013 (2024).
- 100. Ereifej, N. S., Musa, D. B., Oweis, Y. G., Abu-Awwad, M. & Tabnjh, A. K. The influence of core-build up materials on biaxial flexural strength of strength-gradient zirconia and lithium disilicate ceramics: An in-vitro study. *Sci. Rep.* 14, 1–10. https://doi.org/10.1038/s41598-024-82030-5 (2024).
- Huang, J. et al. Optimization design and characteristic of retarding and low-early-strength grouting material for capsule grouting technology: Laboratory and field evaluation. J. Mater. Res. Technol. 19, 4815–4831. https://doi.org/10.1016/j.jmrt.2022.07.038 (2022)
- 102. Palaniappan, M. et al. Synthesis and suitability characterization of microcrystalline cellulose from *Citrus x sinensis* sweet orange peel fruit waste-based biomass for polymer composite applications. *J. Polym. Res.* 31, 105. https://doi.org/10.1007/s10965-024-0 3946-0 (2024).
- 103. Chai, F. et al. Unveiling strength-plasticity synergic mechanism of AZ91 alloy during multi-DOF forming. *J. Mater. Sci. Technol.* **195**, 80–92. https://doi.org/10.1016/j.jmst.2024.02.004 (2024).
- 104. Xiao, Z. et al. Research on the fatigue performance of continuous beam bridges with vibration-mixed steel fiber-reinforced concrete. Sci. Rep. 14, 1–18. https://doi.org/10.1038/s41598-024-79739-8 (2024).
- 105. Shi, Q. et al. Quantitative method for the probability of structural damage based on moment theory. Alex. Eng. J. 108, 984–998. https://doi.org/10.1016/j.aej.2024.09.076 (2024).
- 106. Dong, Y., Yu, H., Feng, Y. & Feng, W. Structure, properties and applications of multi-functional thermally conductive polymer composites. J. Mater. Sci. Technol. https://doi.org/10.1016/j.jmst.2024.02.070 (2024).
- 107. Alagesan, P. K. et al. Comparison of the lateral crushing response of thin-walled aluminum-thermoplastic polymer composite cylindrical shells. *Mech. Adv. Mater. Struct.* https://doi.org/10.1080/15376494.2024.2398732 (2024).
- 108. Khodayari, A., Rehmat, S., Valikhani, A. & Azizinamini, A. Experimental study of reinforced concrete T-beam retrofitted with ultra-high-performance concrete under cyclic and ultimate flexural loading. *Materials* 16, 7595. https://doi.org/10.3390/ma1624 7595 (2023).
- 109. Hoseinzadeh, F., Zabihzadeh, S. M. & Dastoorian, F. Creep behavior of heat-treated beech wood and the relation to its chemical structure. *Constr. Build. Mater.* 226, 220–226. https://doi.org/10.1016/j.conbuildmat.2019.07.181 (2019).
- 110. Xiao, Z. et al. Unexpected effects on creep resistance of an extruded Mg-Bi alloy by Zn and Ca co-addition: Experimental studies and first-principles calculations. J. Mater. Sci. Technol. 201, 166–186. https://doi.org/10.1016/j.jmst.2024.01.083 (2024).
- 111. Wang, J. et al. Influence of basalt fiber on pore structure, mechanical performance and damage evolution of cemented tailings backfill. J. Mater. Res. Technol. 27, 5227–5242. https://doi.org/10.1016/j.jmrt.2023.10.240 (2023).
- 112. Rashid, B., Razali, N., Leman, Z. & Jawaid, M. Single fiber test behavior of lignocellulose sugar palm fibers: Effect of treatments. *Key Eng. Mater.* **925**, 37–46. https://doi.org/10.4028/p-58u653 (2022).
- 113. Rafieizonooz, M. et al. Performances and properties of steel and composite prestressed tendons—A review. *Heliyon*. https://doi.org/10.1016/j.heliyon.2024.e31720 (2024).
- 114. Li, Y. et al. Evaluation of the stress corrosion crack growth behaviour of high-strength marine steel based on model of crack tip mechano-electrochemical effect. J. Mater. Sci. Technol. 190, 93–105. https://doi.org/10.1016/j.jmst.2023.12.007 (2024).

- 115. Ayensa, A. et al. Influence of the flanges width and thickness on the shear strength of reinforced concrete beams with T-shaped cross section. Eng. Struct. 188, 506-518. https://doi.org/10.1016/j.engstruct.2019.03.057 (2019)
- 116. Chan, K. Y. et al. Graphene oxide thin film structural dielectric capacitors for aviation static electricity harvesting and storage. Compos. Part B: Eng. 201, 108375. https://doi.org/10.1016/j.compositesb.2020.108375 (2020).
- 117. Yuan, Y. et al. Flame-retardant epoxy thermosets derived from renewable resources: Research development and future perspectives. J. Mater. Sci. Technol. https://doi.org/10.1016/j.jmst.2024.02.006 (2024).
- 118. Bhattacharya, S., Kalita, K., Čep, R. & Chakraborty, S. A comparative analysis on prediction performance of regression models during machining of composite materials. Materials 14, 6689. https://doi.org/10.3390/ma14216689 (2021).
- 119. Barbero, E., Fernández-Sáez, J. & Navarro, C. Statistical analysis of the mechanical properties of composite materials. Compos. Part B: Eng. 31, 375-381. https://doi.org/10.1016/S1359-8368(00)00027-5 (2000).

Acknowledgements

This research work was funded by Universiti Putra Malaysia (UPM) for financial support under Geran Inisiatif Putra Siswazah (GP-IPS): GP-IPS/2023/9743400 to carry out all research activities. The authors are also very thankful to Department of Aerospace Engineering, Faculty of Engineering, UPM and Aerospace Malaysia Research Centre (AMRC), UPM for providing space and facilities for the project.

Author contributions

V.N. Sukumaar wrote the main manuscript text, create concept methodology, collect and analyse data. M.R. Ishak was the research leader and supervisor with funding contribution for the research activity. M.N. Abdullah provided insights on investigation strategies and outcomes. M.Y.M. Zhuri provided support in software utilisation and visualisations of results, M.R.M. Asyraf gave critical information on previous research drawbacks and basic conceptual ideas. All authors reviewed the manuscript.

Declarations

Competing interests

The authors declare no competing interests.

Additional information

Correspondence and requests for materials should be addressed to V.N.S. or M.R.I.

Reprints and permissions information is available at www.nature.com/reprints.

| https://doi.org/10.1038/s41598-025-00732-w

Publisher's note Springer Nature remains neutral with regard to jurisdictional claims in published maps and institutional affiliations.

Open Access This article is licensed under a Creative Commons Attribution-NonCommercial-NoDerivatives 4.0 International License, which permits any non-commercial use, sharing, distribution and reproduction in any medium or format, as long as you give appropriate credit to the original author(s) and the source, provide a link to the Creative Commons licence, and indicate if you modified the licensed material. You do not have permission under this licence to share adapted material derived from this article or parts of it. The images or other third party material in this article are included in the article's Creative Commons licence, unless indicated otherwise in a credit line to the material. If material is not included in the article's Creative Commons licence and your intended use is not permitted by statutory regulation or exceeds the permitted use, you will need to obtain permission directly from the copyright holder. To view a copy of this licence, visit http://creativecommo ns.org/licenses/by-nc-nd/4.0/.

© The Author(s) 2025